THE ASTROPHYSICAL JOURNAL, 412:34–55, 1993 July 20

ON THE PHOTOIONIZATION OF THE INTERGALACTIC MEDIUM BY QUASARS AT HIGH REDSHIFT

AVERY MEIKSIN
Canadian Institute for Theoretical Astrophysics, University of Toronto, Toronto, ON, Canada M5S 1A1
AND
PIERO MADAU
Space Telescope Science Institute, 3700 San Martin Drive, Baltimore, MD 21218
Received 1992 September 3; accepted 1993 January 26

ABSTRACT

We discuss the reionization of the intergalactic medium (IGM) by quasars at high redshift. We compute the integrated UV background from observed QSOs, taking into account the hydrogen opacity associated with intervening Lyα clouds and Lyman limit systems. We note that the published data appear to indicate a significant underdensity of absorption systems in the Lyα forest with column densities $N_{\rm H\,I} > 10^{15}$ cm^{-2}. This deficit, if real, would result in a reduction of the opacity of the universe at high redshift by a factor of 1.5–3 relative to previous estimates. The QSO contribution over the range $z = 3$–5 to the metagalactic flux at 912 Å may then be as large as $6[(1+z)/4.5]^{0.5} \times 10^{-22}$ ergs cm^{-2} s^{-1} Hz^{-1} sr^{-1} for $q_0 = 0$, and 3×10^{-22} ergs cm^{-2} s^{-1} Hz^{-1} sr^{-1} for $q_0 = 0.5$. We show that this ionizing flux is consistent with current 1 σ upper limits to the Gunn-Peterson optical depth $\tau_{\rm GP}$ at $z \simeq 3$ if the density of the diffuse component of the IGM satisfies $\Omega_D h_{50}^2 \lesssim 0.02$. Models based on QSO photoionization can generate a value of $\tau_{\rm GP} < 0.1$ at $z \gtrsim 3.8$ only in the case of a highly clumped medium. We argue that the Lyα forest may contain a large fraction of the baryons in the universe and estimate the corresponding mass density parameter to be in the range $0.002 < \Omega_{\rm Ly\alpha} h_{50} < 0.05$. We also set constraints on an alternative scenario in which the "intercloud" medium is collisionally ionized, and QSOs photoionize the Lyα forest alone. We conclude that, within the uncertainties, the observed QSOs can provide the required number of ionizing photons at early epochs in several of the models examined.

If quasars turn on suddenly, the universe will be completely photoionized within $\Delta z \lesssim 0.5$ of the turn-on redshift. If instead, QSOs turn on gradually, the associated H II regions may not have fully percolated until $z \sim 5$–5.5. We argue that a new class of absorption systems, arising from intervening patches of neutral unprocessed material which have not yet been engulfed by an H II region, could be observed in the spectra of QSOs just beyond this breakthrough epoch. We estimate their typical H I column densities, sizes, and velocity widths to be 10^{18}–10^{20} cm^{-2}, 0.1–1 Mpc, and 100–1000 km s^{-1}. The patches are expected to persist as distinct absorption features over an extended redshift interval of width $\Delta z \sim 0.5$–1. Eventually, the increase of the equivalent widths of the lines with redshift results in their collective formation of a Gunn-Peterson absorption trough shortward of the Lyα emission line. We find that, for most successful models, the patches appear when $\tau_{\rm GP}$ is still less than unity. Because of the difficulty of measuring such small optical depths at high z, due to the presence of the Lyα forest, neutral patches along the line of sight may provide the first unambiguous detection of a diffuse, primordial IGM. The appearance of these systems would be a sensitive probe of the epoch of reionization. We also discuss the radio signatures of the lines.

Although our emphasis is on the photoionization of the IGM by QSOs, the formalism we develop, including the effects of UV attenuation by intervening absorption systems, as well as many of our results, applies to any discrete source of photoionizing radiation of known number density, intensity, and spectrum.

Subject headings: cosmology: observations — intergalactic medium — quasars: general

1. INTRODUCTION

In the past few years, the growing number of observed quasars with $z > 4$ (Schneider, Schmidt, & Gunn 1989) has promoted a renewed interest in the topic of the reionization of the universe. The absence of an absorption trough on the blue side of the Lyα emission line in the spectra of these high-redshift QSOs requires the diffuse component of the IGM to have been highly ionized by $z \simeq 5$ (Schneider, Schmidt, & Gunn 1991b). The nature of the metagalactic ionizing flux has been the subject of much recent effort (Bechtold et al. 1987; Shapiro & Giroux 1987; Donahue & Shull 1987; Songaila, Cowie, & Lilly 1990; Miralda-Escudé & Ostriker 1990; Madau 1992, hereafter M92; Miralda-Escudé & Ostriker 1992; Fall & Pei 1993), with QSOs and star-forming galaxies as the most plausible candidate sources of photoionization.

It is the purpose of this paper to focus on QSOs detected in optical surveys as the prime source of the metagalactic ionizing flux. The key quantity here is J_{912}, the *mean* specific intensity of the diffuse radiation field at the hydrogen Lyman edge $\nu_{\rm L} = c/912$ Å, as seen by an observer at redshift $z_{\rm obs}$:

$$J_{912}(z_{\rm obs}) = \frac{c}{4\pi H_0} \int_{z_{\rm obs}}^{z_{\rm max}} \frac{(1+z_{\rm obs})^3}{(1+z)^3} \times \frac{\epsilon(\nu, z) \exp\left[-\tau_{\rm eff}(912, z_{\rm obs}, z)\right]}{(1+z)^2(1+2q_0 z)^{1/2}}\, dz\,, \quad (1)$$

where $\epsilon(\nu, z)$ is the proper volume emissivity (ergs cm^{-3} s^{-1} Hz^{-1}) of QSOs at frequency $\nu = \nu_L(1 + z)/(1 + z_{obs})$ and redshift z, $H_0 = 50\ h_{50}$ km s^{-1} Mpc^{-1}, and $\exp[-\tau_{eff}(912, z_{obs}, z)]$ is the transmission of a clumpy medium averaged over all lines of sight. There are two major uncertainties in assessing the contribution of quasars to the ultraviolet extra galactic background at high redshift: (1) the existence and amount of a decline at the faint end of the QSO luminosity function for $z \gtrsim 3$ is still controversial (Boyle 1991; Irwin, McMahon, & Hazard 1991; Schmidt, Schneider, & Gunn 1991; Warren, Hewett, & Osmer 1991); and (2) the estimated continuum opacity of intervening systems is sensitive to the poorly known distributions in redshift and column density of absorption clouds (e.g., Sargent, Steidel, & Boksenberg 1989; Lanzetta 1991). The quasar counts are further made uncertain by the possible bias introduced by dust obscuration arising from intervening systems (Ostriker & Heisler 1984; Wright 1990; Fall & Pei 1993). The decline in the quasar counts at high redshift has been the subject of a long-standing debate. As spectroscopic deep searches (Osmer 1982; Schmidt, Schneider, & Gunn 1986) have suggested a steep decline in the comoving space density of QSOs at $z \gtrsim 2.5$, the prevailing view has been that the observed quasar population cannot provide the number of ionizing photons required to satisfy the Gunn-Peterson test at early epochs (Bechtold et al. 1987; Shapiro & Giroux 1987; Miralda-Escudé & Ostriker 1990; but see Donahue & Shull 1987; M92; Miralda-Escudé & Ostriker 1992; and Fall & Pei 1993). Recently, however, the results of several multicolor photographic surveys have begun to revise our understanding of the quasar luminosity function and evolution over the range $2 < z < 4.5$, and questioned the reality and strength of the decline in number counts. In particular, it has been shown by M92 that QSOs may provide a background flux of $J_{912} \simeq 2 \times 10^{-22}$ ergs cm^{-2} s^{-1} Hz^{-1} sr^{-1} at $z \sim 3$, a value which falls only slightly short of the amount needed to satisfy the "proximity effect" (Bajtlik, Duncan, & Ostriker 1988; Lu, Wolfe, & Turnshek 1991).

In this paper, we greatly expand and extend previous analyses of the QSO contribution to the ionizing radiation field. The plans is as follows. In §§ 2–3 we present results on the properties of discrete absorption systems which are necessary to determine the rate of propagation of photoionizing radiation through the intergalactic medium (IGM) and the resulting intensity of the UV background. In § 2 we discuss the cloudy component of the IGM and the role of discrete absorbers in modulating the metagalactic flux. From an analysis of the published data, we show that there appears to be a significant underdensity of Lyα clouds with $N_{HI} > 10^{15}$ cm^{-2}. This deficit results in a reduction of the effective opacity $\tau_{eff}(912, z_{obs}, z)$ of the universe relative to previous calculations (Miralda-Escudé & Ostriker 1990; M92; Miralda-Escudé & Ostriker 1992), which were therefore underestimating the ionizing background resulting from a given QSO (or blue galaxy) volume emissivity. In § 3 we weigh the contribution of intervening clouds to the cosmological mass density parameter and discuss the interesting possibility of a highly clumped medium, in which much of the baryonic material in the universe is bound in discrete systems. In this scenario it is obviously easier to satisfy the Gunn-Peterson constraint on the amount of intervening, uniformly distributed neutral hydrogen (Gunn & Peterson 1965). In § 4 we analyze the role of clumping in the growth of individual cosmological H II regions and introduce a formalism which relates the background radiation field to the two central quantities describing the ionization state of the IGM: the Gunn-Peterson optical depth and the porosity parameter associated with discrete sources of photoionizing radiation. In § 5 we discuss the constraints on these two quantities inferred from the observations of individual QSOs at high redshifts. In § 6 we reexamine the contribution of the quasar population to the diffuse ionizing flux and show that J_{912} at $z = 3$–5 may be as large as $6[(1 + z)/4.5]^{0.5} \times 10^{-22}$ ergs cm^{-2} s^{-1} Hz^{-1} sr^{-1} for $q_0 = 0$, and 3×10^{-22} ergs cm^{-2} s^{-1} Hz^{-1} sr^{-1} for $q_0 = 0.5$. This estimate is based on objects actually detected in optical surveys. In § 7 we describe the properties of a new class of absorption lines which will arise in the spectra of QSOs, prior to the epoch of complete reionization, from intervening patches of neutral IGM. We derive expressions for the sizes, column and number densities, and line profiles of these features as a function of redshift and discuss the expected 21 cm signature. The appearance of these systems would set constraints on the breakthrough epoch and provide a direct estimate of the density and composition of the primordial, diffuse IGM. In § 8, we discuss the possible contribution of faint blue galaxies to the background ionizing radiation field. This is highly uncertain, since observations of the colors and luminosities of the highest redshift galaxies are limited to a handful of very bright, likely unrepresentative, objects (see, e.g., Chambers, Miley, & Van Breugel 1990). We therefore characterize our estimate by the fraction of the galaxy population turning on at $z \sim 3$, from which UV photons emitted by massive stars can escape into the intergalactic medium without much internal absorption. Finally, we summarize our results in § 9.

2. QUASAR ABSORPTION SYSTEMS

To determine the time scale it takes QSOs to complete the photoionization of the IGM, and the intensity of the resulting metagalactic flux, it is necessary to examine the effects of intervening discrete absorption clouds on the propagation of the ionizing radiation. The role of the absorbers is threefold: (1) before the breakthrough epoch, they retard the growth of individual H II regions; (2) once the H II bubbles overlap, they severely attenuate the radiation from photoionizing sources shortward of the hydrogen Lyman edge; and (3) they absorb a large fraction (>50%) of the flux from individual QSOs shortward of the Lyα emission line, thus complicating an accurate determination of the Lyα optical depth associated with the intercloud medium, a principal constraint for any photoionization model. In the following sections we will discuss the contribution of Lyα clouds and Lyman limit systems to the absorption models. Because of the range in cloud distributions reported in the literature, we will consider three cases, corresponding to low (LA), medium (MA), and high (HA) amounts of attenuation.

2.1. H I *Column Density Distribution*

The Lyα forest is observed to evolve rapidly with redshift. To facilitate a comparison with previous studies (Miralda-Escudé & Ostriker 1990; M92), we shall adopt here:

$$\frac{dN}{dz} = 3.0(1 + z)^{2.4} \qquad (2)$$

for lines with rest equivalent width $W > 0.36$ Å. This value corresponds to $N_{HI} > 1.7 \times 10^{14}$ cm^{-2} if we take an average Doppler parameter of $\langle b \rangle = 35$ km s^{-1} (e.g., Rauch et al.

1992). Equation (2) is based on the analysis of Bajtlik et al. (1988) and is consistent with the more recent determination of Lu et al. (1991). Murdoch et al. (1986) have determined an exponential equivalent width distribution between $0.2 < W < 1.6$ Å, which translates into a power-law neutral hydrogen column density distribution of the form

$$\frac{dN}{dN_{\rm H\,I}} \propto N_{\rm H\,I}^{-\beta}\,, \tag{3}$$

with $\beta = 1.5$–1.8 (Carswell et al. 1984; Tytler 1987; Carswell et al. 1987). There is very limited information on the high column density tail. The results of Murdoch et al. suggest continuity in the Lyα forest through values of 10^{15}–10^{17} cm^{-2}, but the data covering this range are sparse and uncertain. The critical importance of these clouds lies in the fact that they may absorb as much as half of the metagalactic radiation field arising from discrete sources.

It has been suggested by Steidel (1991) that there may be far fewer Lyα clouds with optical depth just below unity at the Lyman edge than is indicated by equation (3), and that this deficit would result in substantially less attenuation than predicted on the basis of a single power-law model. In their study of PKS 2000−330, Carswell et al. (1987) had also expressed concern that a single power law may not adequately describe the distribution of column densities. They found a best-fit value of $\beta = 1.71$ for systems with $\log N_{\rm H\,I} > 13.75$, but also noted that the fit was rejected at the 96% confidence level. The failure of the single power-law model was apparently a result of a steepening in the distribution at the high column density end, with a break occurring at $\log N_{\rm H\,I} \simeq 14.35$.

In this section we assess the number density of Lyα clouds for $\log N_{\rm H\,I} > 15$, the domain that contributes most to the attenuation, using the tabulations of column densities available in the literature. There are four quasars with observations of sufficient resolution and signal-to-noise suitable for our purpose, and with reported column densities complete above some threshold. These are Q0420−388 (Atwood, Baldwin, & Carswell 1985), PKS 2000−330 (Carswell et al 1987), Q1100−264 (Carswell et al. 1991), and Q0014+813 (Rauch et al. 1992). In the case of Q0420−388, we adopt the criteria of Atwood et al. sample A: we consider only unblended Lyα lines with column densities and b parameters determined using members of the Lyman series in addition to Lyα. This results in 29 lines with $z > 2.72$. We find $\langle b \rangle = 30 \pm 2$ km s^{-1} and $\beta = 2.0 \pm 0.2$, in agreement with the values quoted by Atwood et al. The reported completeness limits for the column density distributions are $\log N_{\rm H\,I} = 13.75$ for Q0420−388, $\log N_{\rm H\,I} = 13.75$ for PKS 2000−330, $\log N_{\rm H\,I} = 13.0$ for Q1100−264, and $\log N_{\rm H\,I} = 13.3$ for Q0014+813. Atwood et al. find $\beta = 2.03 \pm 0.25$ in Q0420−388. From Q1100−264, Carswell et al. (1991) find $\beta = 1.7 \pm 0.1$, while Rauch et al. (1992) find $\beta = 1.74 \pm 0.06$ from Q0014+813. In contrast to the PKS 2000−330 case, none of these single power-law fits can be statistically rejected.

We combine the data for the four systems, and require $\log N_{\rm H\,I} > 13.75$ for completeness. To ensure the reliability of the Lyα tabulations, we enforce a few further requirements. We remove Lyα lines associated with metal systems, based on the report of metal-line detections in the original observations or in the C IV surveys of Sargent, Boksenberg, & Steidel (1988), and Steidel (1990a). These metal systems are likely to form a distinct population of absorbers, possibly associated with the halos of intervening galaxies.[1] Following Carswell et al. (1987), we also require $b > 5$ km s^{-1}, as low column density systems with lower b-values would be missed. This result in the loss of just one line, in PKS 2000−330, with $\log N_{\rm H\,I} = 13.96$.

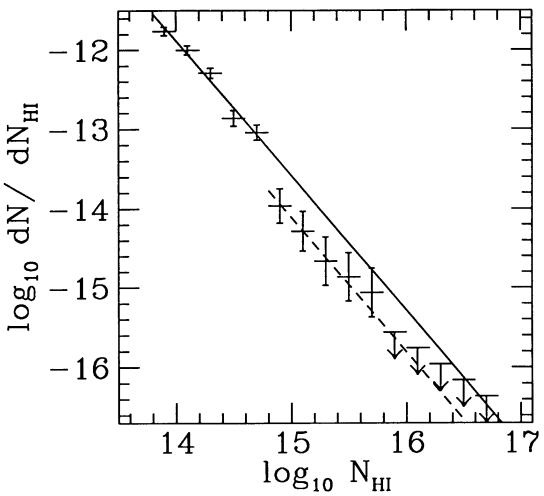

FIG. 1.—Lyα forest H I column density distribution, compiled from high-resolution observations of four QSOs. A deficit of absorbers by a factor of 3, significant at the 4 σ level, is apparent in the range $15 < \log N_{\rm H\,I} < 16$. No Ly$\alpha$ forest lines occur for $\log N_{\rm H\,I} > 16$, with a significance of 3 σ. The solid line is the maximum likelihood fit over the range $13.75 < \log N_{\rm H\,I} < 14.8$, for which $\beta = 1.7$. The dashed line is for $\beta = 1.7$, normalized to the systems in the range $14.8 < \log N_{\rm H\,I} < 16$.

In the combined sample we find 230 lines in the range $13.75 \leq \log N_{\rm H\,I} < 15$. From equation (3), the predicted number of systems with $15 < \log N_{\rm H\,I} < 17$ is 34.1 for $\beta = 1.7$. Only nine lines are detected. The probability of so few detections is 3.6×10^{-7}. (There would actually be 12 detections, if the Lyα lines associated with metal complexes were included. The probability of observing as few as 12 lines is 1.2×10^{-5}.) All nine systems have $\log N_{\rm H\,I} < 16$. The number of systems expected in the range $15 < \log N_{\rm H\,I} < 16$ is 28.4. The probability of detecting as few as nine lines is 2.2×10^{-5}. The probability of observing no lines in the range $16 < \log N_{\rm H\,I} < 17$, compared to an expected number of 5.7, is 3.3×10^{-3}. Therefore, despite the apparent acceptability of the fits with $\beta = 1.7$, there is a highly significant deficit of lines with $\log N_{\rm H\,I} > 15$, extending at least up to $\log N_{\rm H\,I} = 17$. This is clearly seen in the histogram of the combined line counts for the four QSOs under study, shown in Figure 1. No lines are found for

[1] The metal-line criterion results in the removal of a complex of lines in the spectrum of Q0420−388, associated with a damped Lyα system candidate centered at $z = 3.0857$. In Q1100−264, a complex associated with another damped candidate at $z = 1.84$ is removed as well (see Carswell et al. 1991). Also excluded are the three Lyα lines in the $z = 3.33$ metal complex in PKS 2000−330 ($\log N_{\rm H\,I} = 14.41 \pm 0.09$, $\log N_{\rm H\,I} = 14.98 \pm 6.38$, and $\log N_{\rm H\,I} = 16.04 \pm 6.29$), and three lines in Q0014+813 at $z = 2.7996$ ($\log N_{\rm H\,I} = 16.40 \pm 0.20$), $z = 3.2266$ ($\log N_{\rm H\,I} = 15.13 \pm 0.35$), and $z = 3.2274$ ($\log N_{\rm H\,I} = 15.49 \pm 0.26$). We note an apparent discrepancy between the observations of Q0014+813 by Sargent et al. (1989) and Rauch et al. (1992). Sargent et al. find a Lyman limit system at $z = 2.813$ with a column density of $\log N_{\rm H\,I} = 17.40$. The corresponding Ly$\alpha$ feature is the $z = 2.7996$ system found by Rauch et al., with $\log N_{\rm H\,I} = 16.40 \pm 0.20$ and $b = 89 \pm 4$ km s^{-1}. To match the rest equivalent width of 1.77 Å measured by Rauch et al. to the column density measured by Sargent et al. a value of $b = 75$ km s^{-1} is required. Therefore, in this column density range (where estimates are especially difficult because of the extreme flatness of the curve of growth), the error bars in Rauch et al. may have been underestimated.

log $N_{\rm H\,I} > 15.8$. An apparent decrement by a factor ~ 4 occurs between log $N_{\rm H\,I} = 14.7$ and 14.9. A maximum likelihood fit to the data for log $N_{\rm H\,I} > 13.75$ yields $\beta = 1.98 \pm 0.07$. The fit is rejected by a K-S test with 98% confidence. Limiting the column density range to $13.75 < \log N_{\rm H\,I} < 15.8$ gives $\beta = 1.92 \pm 0.06$, which is again rejected at the 93% level. An acceptable fit is obtained over the range $13.75 < \log N_{\rm H\,I} < 14.8$ with $\beta = 1.69 \pm 0.04$. Taking $\beta = 1.7$, the projected number of systems in the range $14.8 < \log N_{\rm H\,I} < 16$ is 44. The number of systems detected is 13, again short by a factor of 3.4.

In principle, biases in the column density determinations could be introduced by the data analysis procedure. We may check for biases using the results of the simulation by Rauch et al. (1992) designed to test the effects of instrumental resolution and noise on their line-fitting procedure. We find from inspection of their Figure 6 that they accurately reproduce the input distribution in the region of the deficit. The number of lines expected with $(14.3, 15) < \log N_{\rm H\,I} < 15.7$ is (9.2, 3.4), while (13, 3) are found. Further simulations, however, would be highly desirable. As another check on any biases, we perform a second analysis on a subsample of the above lines meeting the criteria of Atwood et al. sample A for Q0420−388. This subsample avoids blended lines and has more reliable determinations of the H I column densities since higher order members of the Lyman series are used as constraints. In addition to the 29 lines in Q0420−388, we find 28 lines in PKS 2000−330 and two lines in Q0014−813. (No lines which satisfy these criteria are available in Q1100−264.) Combining the data for these three QSOs, we find 33 lines in the range $13.75 < \log N_{\rm H\,I} < 15$. The best-fit power law for the column density distribution over this range gives $\beta = 1.71 \pm 0.13$. The expected number of lines with log $N_{\rm H\,I} > 15$ is 5.08 for $\beta = 1.7$, while no lines are found. The probability of finding no lines is 0.0062. Again, the deficit of high column density systems is statistically significant.

The underdensity of lines with log $N_{\rm H\,I} \gtrsim 15$, and the absence of log $N_{\rm H\,I} > 16$ systems is somewhat surprising. A break may have been expected near log $N_{\rm H\,I} = 17.2$, where clouds become optically thick at the Lyman edge. Considerations of the Jeans mass of the clouds, however, suggest that a break at log $N_{\rm H\,I} \gtrsim 15$ may arise naturally as a consequence of the onset of gravitational instabilities. We discuss this interpretation in § 3 below.

The evolution of the Lyman limit systems at high redshift is currently controversial. Sargent et al. (1989) obtain for clouds with $\tau_{\rm L} \geq 1.5$, where $\tau_{\rm L}$ is the optical depth at the Lyman edge:

$$\frac{dN}{dz} \simeq 0.75(1+z)^{0.68 \pm 0.54}, \quad (4)$$

and $\beta = 1.39$. Steidel (1992) estimates the number of metal systems at $z \sim 3$ with $16 < \log N_{\rm H\,I} < 17$ to be comparable to the number of Lyman limit systems with $\tau_{\rm L} \geq 1.5$. The inclusion of these $\tau_{\rm L} < 1$ absorbers would decrease the metagalactic flux estimated below by at most 10%–25%. For simplicity, we will consider in the attenuation models only Lyman limit systems with $\tau_{\rm L} \geq 1$.

At $z = 3$, the number density of Lyman limit systems will exceed the number density of Lyα absorbers for $N_{\rm H\,I} = 1.59 \times 10^{17}$ cm^{-2} ($\tau_{\rm L} = 1$), by a factor of 2, if equations (2) and (3) are adopted with $\beta = 1.7$. A deficit in the Lyα forest of a factor of 3 for $N_{\rm H\,I} > 6.3 \times 10^{14}$ cm^{-2} would increase the discrepancy to a factor of 6. In the absence of the deficit, the Lyα forest and Lyman limit systems may be matched at $N_{\rm H\,I} = 1.59 \times 10^{17}$ cm^{-2} if $\beta = 1.5$ is adopted for both systems. The effect of the deficit is to require the Lyα forest column density distribution both to decrease in amplitude by a factor of ~ 3 and to flatten from $\beta = 1.7$ to $\beta = 1.39$ in the range $6.3 \times 10^{14} < N_{\rm H\,I} < 1.59 \times 10^{17}$ cm^{-2} in order to match the Lyman limit density of Sargent et al. (1989).

A different redshift evolution is reported by Lanzetta (1991) for the Lyman limit systems. He fits a double power law to systems with $\tau_{\rm L} \geq 1$ of the form

$$\frac{dN}{dz} \simeq 1.2(1+z)^{0.3 \pm 0.9}, \quad 0.36 < z < 2.5;$$
$$\simeq 8.1 \times 10^{-4}(1+z)^{5.7 \pm 1.9}, \quad 2.5 < z < 3.7, \quad (5)$$

with $\beta = 1.25 \pm 0.03$. This results in a somewhat greater amount of absorption of photoionizing radiation at high redshift. (Note that Steidel 1992 disputes such a steep increase and finds that the weak evolution described in eq. [4] persists to high redshifts.) The rapid evolution case receives a natural interpretation as an extension of the Lyα forest to high column densities. Fixing the z-dependence as $(1+z)^{2.4}$, we fit the bins in Lanzetta's Figure 1 with $z > 1.5$ to obtain

$$\frac{dN}{dz} \simeq 0.086(1+z)^{2.4}, \quad (6)$$

with a reduced $\chi^2 \simeq 1$. This is equivalent to extending equation (2) to column densities in the range 1.59×10^{17}–10^{22} cm^{-2}, with $\beta = 1.52$. We adopt this evolution model for our model HA.

2.2. *Attenuation Models*

2.2.1. *Low Attenuation Model*

For model LA, we adopt equation (3) for the Lyα forest column density distribution with $\beta = 1.7$ and an upper cutoff of 6.3×10^{14} cm^{-2}. Adding additional absorbers up to log $N_{\rm H\,I} = 16$, with a suppression factor of 3 based on the above analysis, would decrease our estimate below for the UV metagalactic flux by only an additional 10%. (The decrease is 10%–25% if the upper limit is extended up to log $N_{\rm H\,I} = 17.2$, again with a suppression factor of 3.) For simplicity, we will therefore assume no systems in the range $14.8 < \log N_{\rm H\,I} < 17.2$ in attenuation model LA. Note that eliminating the Lyα forest altogether would result in only an additional 10%–20% to the total metagalactic flux.

To be consistent with Miralda-Escudé & Ostriker (1990) and M92, for the Lyman limit systems we take

$$\frac{dN}{dz} = 0.96(1+z)^{0.5}, \quad (7)$$

and $\beta = 1.5$. This agrees with equation (4) above within the errors.

2.2.2. *Medium Attenuation Model*

To be consistent with Miralda-Escudé & Ostriker (1990) and M92, we adopt $\beta = 1.5$ and $N_{\rm H\,I} \leq 1.59 \times 10^{17}$ cm^{-2} ($\tau_{\rm L} \leq 1$), for the Lyα forest. We use the same expression for the Lyman limit systems as for model LA. Thus for model MA, $\beta = 1.5$ is adopted over the entire column density range from the Lyα forest through the Lyman limit systems.

2.2.3. *High Attenuation Model*

For model HA, we interpret the rapid evolution of Lyman limit systems in equation (6) as an extension of the Lyα cloud distribution into the damped Lyα systems domain, $N_{\rm H\,I} \leq 10^{22}$

TABLE 1

ABSORPTION CLOUD MODELS

Model	A_0	γ	β	$N_{\rm H\,I}$ Range
Lyα Forest: $\frac{\partial^2 N}{\partial z\,\partial N_{\rm H\,I,14}} = A_0(1+z)^{\gamma} N_{\rm H\,I,14}^{-\beta}$				
LA	3.04	2.4	1.70	$10^{14} < N_{\rm H\,I} < 6.3 \times 10^{14}$ cm^{-2}
MA	1.96	2.4	1.50	$10^{14} < N_{\rm H\,I} < 1.59 \times 10^{17}$ cm^{-2}
HA	2.06	2.4	1.52	$10^{14} < N_{\rm H\,I} < 10^{22}$ cm^{-2}
Lyman Limit Systems: $\frac{\partial^2 N}{\partial z\,\partial N_{\rm H\,I,17}} = A_0(1+z)^{\gamma} N_{\rm H\,I,17}^{-\beta}$				
LA	0.74	0.5	1.50	$1.59 \times 10^{17} < N_{\rm H\,I} < 10^{22}$ cm^{-2}
MA	0.74	0.5	1.50	$1.59 \times 10^{17} < N_{\rm H\,I} < 10^{22}$ cm^{-2}
HA	0	...	...	...

cm^{-2}. To provide the correct number of observed Lyman limit systems we take $\beta = 1.52$ over the range $10^{14} < N_{\rm H\,I} < 10^{22}$ cm^{-2}.

The attenuation models adopted are summarized in Table 1.

2.3. H I *Photoelectric Absorption*

The photoelectric absorption by H I associated with Poisson-distributed Lyα clouds and Lyman limit systems is described by the transmission term in equation (1), where the effective optical depth is given by

$$\tau_{\rm eff}(912, z_{\rm obs}, z) = \int_{z_{\rm obs}}^{z}\int_{0}^{\infty} \frac{\partial^2 N}{\partial N_{\rm H\,I}\,\partial z'} \times [1 - \exp(-N_{\rm H\,I}\sigma_{\nu'})]dN_{\rm H\,I}dz' , \quad (8)$$

(e.g., Paresce, McKee, & Bowyer 1980). Here $\nu' = \nu_L(1+z')/(1+z_{\rm obs})$, and $\sigma_{\nu'}$ is the hydrogen photoionization cross section. Photons observed at the hydrogen Lyman edge will not undergo He II absorption on their way if $1 + z < 4(1 + z_{\rm obs})$. The He I contribution to the attenuation is found to be negligible in the case of a QSO-dominated background. An approximate (within 15%) integration of equation (8) yields for the low absorption model LA:

$$\tau_{\rm eff}^{\rm LA}(912, z_{\rm obs}, z) \simeq 0.0118x_{\rm obs}^3(x^{0.4} - x_{\rm obs}^{0.4}) + 2.35x_{\rm obs}^{1.5}\ln\left(\frac{x}{x_{\rm obs}}\right) - 0.78x_{\rm obs}^3(x_{\rm obs}^{-1.5} - x^{-1.5}) - 0.003(x^{1.5} - x_{\rm obs}^{1.5}) , \quad (9)$$

where $x_{\rm obs} = 1 + z_{\rm obs}$, and $x = 1 + z$. The first term on the right-hand-side represents the contribution of Lyα clouds, the others are due to Lyman limit systems. In model LA, the deficit of optically thin clouds with $N_{\rm H\,I} > 10^{15}$ cm^{-2} reduces the contribution of the Lyα forest to $\lesssim 10\%$ of the total opacity. Model MA is characterized by the same expression as model LA, except that the coefficient of the first term is now 0.244 (M92). This results in an increase in the total opacity by a factor ranging from 1.6 to 3.1 for $2 \le z \le 5$. At $z \sim 1$, the optical depth associated with model MA is only 30% larger than in model LA, as Lyman limit systems dominate the opacity of the universe. In the high-absorption model HA we find instead

$$\tau_{\rm eff}^{\rm HA}(912, z_{\rm obs}, z) \simeq 0.097x_{\rm obs}^{1.56}(x^{1.84} - x_{\rm obs}^{1.84}) - 0.0068x_{\rm obs}^3(x^{0.4} - x_{\rm obs}^{0.4}) - 8.06 \times 10^{-5}(x^{3.4} - x_{\rm obs}^{3.4}) . \quad (10)$$

A comparison shows that $\tau_{\rm eff}^{\rm HA}$ yields the smallest attenuation for $z < 1.5$, and the largest for $z > 3$.

3. THE TOTAL BARYONIC CONTENT OF THE IGM

Whether or not QSOs may provide a UV background of adequate intensity to satisfy the Gunn-Peterson test at high redshift depends on the baryonic content of the IGM. In this section we will estimate the amount of baryonic material which must be photoionized and argue that a large fraction of these baryons may reside in the Lyα forest. The damped Lyα and Lyman limit systems are believed to be sparse enough that their covering factor about an H II region is negligible even for a source as intense as a QSO, and their contribution to the clumping factor in the propagation of an individual H II region (before the breakthrough epoch) may be neglected. In the following, the only role of the Lyman limit systems we will consider is in attenuating the UV background once the reionization of the IGM is completed, as discussed in § 2.

We estimate the baryonic density parameter of the photoionized IGM, $\Omega_{\rm IGM}$, to be the difference between Ω_b, the total cosmological baryonic density of the universe, and the baryonic mass bound in discrete objects, Ω_A, which does not include the Lyα cloud phase of density $\Omega_{\rm Ly\alpha}$. The latter is defined to be a part of the intergalactic medium, together with a diffuse component of density Ω_D, $\Omega_{\rm IGM} = \Omega_D + \Omega_{\rm Ly\alpha}$. For the cosmological density parameter, we adopt the nucleosynthesis constrained value of Walker et al. (1991), $\Omega_b h_{50}^2 = 0.05 \pm 0.01$.

The available data on the Lyα forest do not constrain $\Omega_{\rm Ly\alpha}$ very tightly. If we assume photoionization equilibrium with the diffuse field, the total hydrogen gas density $n_{\rm H,c}$ of a spherical cloud of average H I column density 10^{14} cm^{-2} is related to its diameter D_{14} by

$$n_{\rm H,c}(z) = \left[\frac{3}{2}\frac{G_{\rm H}J_{912}(z)(10^{14}\ {\rm cm}^{-2})}{(1+2\chi)\alpha_{\rm A}(T)D_{14}}\right]^{1/2} \simeq 5.3 \times 10^{-5}\left[\frac{D_{14}(z)}{20\ {\rm kpc}}\right]^{-1/2} J_{-22}^{1/2}(z)\ {\rm cm}^{-3} , \quad (11)$$

where $J_{912}(z) = J_{-22}(z) \times 10^{-22}$ ergs cm^{-2} s^{-1} Hz^{-1} sr^{-1} is the metagalactic flux, $G_{\rm H}$ is the ionization efficiency

$$G_{\rm H} \equiv \int_{\nu_L}^{\infty} (4\pi J_\nu \sigma_\nu / h_P)(d\nu/\nu)/J_{912} , \quad (12)$$

$\alpha_{\rm A} \simeq 4.2 \times 10^{-13} T_4^{-0.75}$ cm^3 s^{-1} is the recombination coefficient to all levels of hydrogen (Osterbrock 1989), and $T = T_4 \times 10^4$ K is the cloud temperature. We take $T_4 = 2$, a number ratio of helium to hydrogen of $\chi = 1/12$, and a spectral index of 0.5 in equation (12) (cf. M92). Note that we include a geometric factor of $\frac{2}{3}$ here and below in the expression for the average (over all lines of sight) column density $\langle N_{\rm H\,I}\rangle$ through a cloud of diameter D, $\langle N_{\rm H\,I}\rangle = (\frac{2}{3})n_{\rm H\,I}D$. From equation (2), the volume filling factor f_c of this subpopulation of the Lyα forest is $f_c \sim 3(2H_0 D_{14}/3c)(1+z)^{4.4}(1+2q_0 z)^{1/2}$. If we define the closure hydrogen density as $n_{\rm H,crit}(0) = 3H_0^2/[8\pi G m_{\rm H}(1+4\chi)] = 2.11 \times 10^{-6}\ h_{50}^2$ cm^{-3}, we find for

$\Omega_{\rm Ly\alpha} = f_c\, n_{\rm H,c}/n_{\rm H,crit}$:

$$\Omega_{\rm Ly\alpha} \sim 0.002\, h_{50}^{-1}\left(J_{-22}\frac{D_{14}}{20\ {\rm kpc}}\right)^{1/2}, \quad (13)$$

where we have normalized at $z = 2.5$ and assumed $q_0 = 0.5$. We will show below that quasers may generate a flux $J_{-22} \gtrsim 2$ at these redshifts. If 10^{14} cm^{-2} Lyα clouds have diameters as large as 200 kpc, their contribution to the closure density may therefore be as high as $\Omega_{\rm Ly\alpha} \sim 0.008$.

In order to estimate the contribution of the Lyα forest to $\Omega_{\rm Ly\alpha}$ over the entire range of column densities, we shall consider two specific models. First, the clouds are taken to be confined by the pressure of the diffuse component, a model which is motivated by the possibility of a collisionally ionized, hot ($T \sim 10^6$ K), and rarefied intercloud medium (Sargent et al. 1980). Photoionization by discrete sources is still necessary in this scenario to maintain the high ionization state of the "cold" ($T \sim 10^4$ K) and denser absorbers, and we will investigate in § 6 below whether the observed quasars are capable of meeting this requirement. (Pressure confinement could not be achieved without collisional ionization, as photoionization yields a temperature which is nearly independent of density.) In the second model the clouds are not confined and expand at a constant rate. If the Doppler parameter ($\langle b\rangle = 35$ km s^{-1}) is a measure of the expansion bulk speed, then the expanding clouds will all have the same size at a given epoch, with a diameter on the order of $\langle b\rangle[H_0(1+z)(1+2q_0 z)^{1/2}]^{-1} \sim$ 100–200 h_{50}^{-1} kpc at $z = 2.5$. We describe the results of our analyses in Appendix A.

For pressure-confined clouds, the total mass density is dominated by the most massive, hence highest column density, systems. Clouds created at the high end of the size range are not expected to survive. The Jeans instability criterion yields a maximum diameter, thus a maximum column density:

$$\langle N_{\rm H\,I}\rangle_{\rm max} \simeq 2.0\times 10^{16}\left(\frac{D}{200\ {\rm kpc}}\right)^{-3} {\rm J}_{-22}^{-1}\ {\rm cm}^{-2}. \quad (14)$$

Absorbers with log $N_{\rm H\,I} \sim 14$ have sizes of at least 10 h_{50}^{-1} kpc at $z \sim 2.5$ (Smette et al. 1991). Thus, in the pressure-confined model, we scale by $D_{14} \simeq 20(\langle N_{\rm H\,I}\rangle/10^{14}\ {\rm cm}^{-2})$ kpc and estimate

$$\langle N_{\rm H\,I}\rangle_{\rm max} \simeq 2\times 10^{15}\left(\frac{D_{14}}{20\ {\rm kpc}}\right)^{-3/4} {\rm J}_{-22}^{-1/4}\ {\rm cm}^{-2}. \quad (15)$$

This critical column density (corresponding to a diameter of 400 kpc) is close to the value where a break appears to occur in the Lyα forest $N_{\rm H\,I}$ distribution, as discussed in § 2.1.1 above. It is therefore tempting to suggest that we may have detected, in the published data, the signature of the onset of a Jeans instability. We use equations (15) and (A2) in Appendix A to estimate $\Omega_{\rm Ly\alpha}$ in the pressure-confined models. We obtain $0.005 < \Omega_{\rm Ly\alpha} h_{50} < 0.05$.

By contrast, if the clouds expand at a constant rate, the density parameter is dominated by systems with the lowest mass. This is taken to correspond to a minimum average column density of $\langle N_{\rm H\,I}\rangle_{\rm min} = 10^{13}$ cm^{-2} at $z = 2.5$. From equation (A3) in Appendix A we obtain $0.04 < \Omega_{\rm Ly\alpha} h_{50} < 0.07$. We note that for this model, the Jeans instability again imposes a maximum column density, given by equation (14).

Other components include Lyman limit and damped Lyα systems. From photoionization models of optically thick clouds, Steidel (1990b) estimates the mass density associated with Lyman limit systems to be $\Omega_{\rm LLS} \sim 8\ h_{50}^{-1} \times 10^{-3}$, while Lanzetta et al. (1991) estimate $\Omega_{\rm DLA} \simeq 1.6 - 3.0\ h_{50}^{-1} \times 10^{-3}$ for the damped systems. In a separate analysis, Fall & Pei (1993) find a density a factor of 2 larger for the damped systems. The total baryonic density $\Omega_A = \Omega_{\rm LLS} + \Omega_{\rm DLA}$ in these high column density absorbers is therefore likely to be $\Omega_A h_{50} \sim 0.01$–$0.02$. Clusters of galaxies may also retain a large fraction of baryons. If $\Omega_{\rm clust}$ is dominated by Abell richness class 2 clusters, with Coma as typical ($M_{\rm gas} \simeq 5\times 10^{14}\ h_{50}^{-5/2}\ M_\odot$, Hughes 1989), then a space density of $2.9\times 10^{-7}\ h_{50}^3$ Mpc^{-3} (Bahcall 1988) implies $\Omega_{\rm clust}\ h_{50}^{3/2} \sim 2\times 10^{-3}$. If $\Omega_{\rm Ly\alpha}\ h_{50} < 0.01$, we estimate the density of the diffuse intercloud medium, $\Omega_D = \Omega_b - (\Omega_{\rm Ly\alpha} + \Omega_A + \Omega_{\rm clust})$, to be

$$0.01 < \Omega_D < 0.04 \quad (H_0 = 50),$$
$$0.005 < \Omega_D < 0.01 \quad (H_0 = 80). \quad (16)$$

If $\Omega_{\rm Ly\alpha}\ h_{50}$ is greater than few times 10^{-2}, Ω_D may be as low as 10^{-3} (10^{-4}) for $H_0 = 50$ ($H_0 = 80$). Although it may seem more likely for Ω_D to be closer to the higher estimates, the interesting alternative that much of the baryonic material in the universe is bound in the Lyα forest cannot be ruled out. We thus explore in the following two classes of models: (*a*) a smooth medium (model SM) case, in which most of the baryonic material in the IGM is in the form of a uniformly distributed, intercloud component; and (*b*) a clumped medium (model CM) case, in which most of the IGM baryons are contained in the Lyα cloud phase.

4. OVERLAPPING COSMOLOGICAL H II REGIONS

A central quantity describing the ionization state of the IGM in photoionization models is given by the product of the spatial number density of the radiating sources and the volume associated with an individual H II bubble, known as the porosity parameter $Q(z)$. Since every UV photon must be absorbed somewhere in the IGM, the volume filling factor of ionized hydrogen is equal to Q for $Q < 1$. If the ionizing sources are randomly distributed, the H II regions are spatially isolated for $Q \ll 1$, and the IGM ionization process cannot be described as due to a statistically homogeneous radiation field (Arons & Wingert 1972). Overlappings of ionization fronts are common when $Q \lesssim 1$, and the IGM is completely reionized for $Q = 1$. In this section, we will confine our analysis to the regime $Q > 1$, that is to say, after the breakthrough epoch, when all radiation sources can see each other in the hydrogen Lyman continuum. Even in this regime the porosity parameter continues to contain useful information concerning the nature of the photoionizing sources, since it is proportional to the total metagalactic flux. Consequently, given an IGM baryon density, we can relate Q to the Lyα Gunn-Peterson optical depth $\tau_{\rm GP}$.

The evolution of an expanding cosmological ionization front, generated in a multicomponent IGM by an isolated point source of UV radiation, is governed by the equation

$$4\pi r_I^2\, n_{\rm H}\left(\frac{dr_I}{dt} - Hr_I\right) = S(0) - \frac{4}{3}\pi r_I^3 \sum_i (1+2\chi) \times \Omega_i\, n_{{\rm H},i}\, n_{\rm H,crit}\, \alpha_{\rm B}(T_i), \quad (17)$$

where r_I is the proper radius of the I-front, $n_{\rm H} = \sum_i f_i n_{{\rm H},i}$ is the volume-averaged hydrogen density of the IGM, H is the Hubble constant, $S(0)$ is the number of ionizing photons emitted from the central source per unit time, $\alpha_B \simeq$

$2.6 \times 10^{-13}\ T_4^{-0.845}\ \mathrm{cm^3\ s^{-1}}$ is the recombination coefficient to the excited states of hydrogen, and the sum is taken over the various components i of the IGM, each of density parameter Ω_i and filling factor f_i. A fixed He to H number ratio χ is assumed, with both H and He fully ionized. The equation for the evolution of an I-front in a uniform IGM has been derived by Shapiro (1986). We give a formal derivation of the extension to a multicomponent medium in Appendix B.[2] For a medium of sufficiently low density and low clumping factor, the ionization front generated by a QSO or a star-forming galaxy fails to grow to even half of its Strömgren radius (Shapiro & Giroux 1987). In this case radiative recombinations within the H II region may be neglected on the right-hand-side of equation (17) (Madau & Meiksin 1991), an approximation which allows us to simplify our treatment of the reionization process and to use upper limits on the Lyα optical depth to provide direct constraints on the porosity parameter. These analytical results apply to an accuracy of 10% or better in the smooth IGM case (model SM) and permit a direct quantitative assessment of the requirements for reionization without extensive numerical calculations. In this section we provide an expression for the porosity as a function of redshift for two evolution models of the source emissivity: (*a*) sudden turn-on (model CC), where the comoving number density of the radiating sources is assumed to be constant up to the turn-on redshift $z_{\rm on}$; and (*b*) exponential growth with increasing expansion factor (model ED), where we assume instead a constant comoving number density only for $z < z_*$, which then decays exponentially for $z > z_*$. We present a relation between the Lyα optical depth, the IGM density, and the porosity for model SM. Note that in model CM, recombinations in a clumpy medium preclude a simple relation between these quantities.

Accordingly, we take the luminosity function of the radiating sources to be of the form

$$\Phi(L, z) = \Phi_* L_*^{-1} \phi(y) f(z, \tilde{z}) , \tag{18}$$

where $y \equiv L/L_*$, and L_* is a characteristic luminosity. The function $f(z, \tilde{z})$ is defined as

$$f(z, \tilde{z}) = \begin{cases} 1, & z < \tilde{z} ; \\ \exp\,[-\mu(z - \tilde{z})], & z > \tilde{z} , \end{cases} \tag{19}$$

where μ is a decay constant. In model CC, $\tilde{z} = z_{\rm on}$, so $f(z, \tilde{z}) = 1$. In model ED, $\tilde{z} = z_*$. We shall see in § 6 that this functional form mimics fairly well the behavior of QSOs for $2 < z < 5$, the redshift range over which we shall confine our discussion.

In the case of a constant luminosity source which turns on at redshift $z_{\rm on}$, the comoving volume of the H II bubble generated in a $q_0 = 0$ or 0.5 universe is, neglecting recombinations,

$$V_I = \frac{S(0)}{n_{\rm H}(0) H_0} \frac{1}{1 + q_0} \left[(1 + z)^{-(1+q_0)} - (1 + z_{\rm on})^{-(1+q_0)}\right] . \tag{20}$$

[2] The generalization to a clumpy medium by Shapiro & Giroux (1987) contains two misprints. Their initial definition of the clumping factor should read $c_l = \langle n^2\rangle/\langle n\rangle^2$ instead of $[\langle n^2\rangle/\langle n\rangle^2]^{1/2}$. In their discussion of the Lyα forest clouds, Shapiro & Giroux correctly redefine $c_{l,j}$, but another misprint appears in the expression for the recombination rate. In their definition of the parameter λ_j, $n_{{\rm H},i}$ should instead read $n_{{\rm H},i}/\Omega_b$. They use the correct expressions in their calculations.

Therefore, the porosity parameter can be expressed as[3]

$$Q(z) = \Phi_*\left[\frac{L_*}{n_{\rm H}(0) H_0 h_P}\right] \frac{\xi\epsilon}{1 + q_0} (1 + z)^{-(1+q_0)} \times \left[1 - \left(\frac{1 + z}{1 + z_{\rm on}}\right)^{1+q_0}\right] \quad (\mathrm{CC}) , \tag{21}$$

where $\xi = \int_{\nu_L}^{\infty} (\tilde{f}_\nu/\nu) d\nu$ is the dimensionless photon luminosity of the radiating sources,[4] and $\epsilon = \int \phi(y) y\, dy$ is the dimensionless volume emissivity.

In Appendix C we present an analytical expression for $Q(z)$ in the exponential decay ED evolution model. In this model, the resulting metagalactic flux at frequency ν and epoch $z > z_*$ is

$$J(\nu, z) = \frac{c}{4\pi H_0} \Phi_* L_* \epsilon \tilde{f}_\nu f(z, z_*) \mathscr{J}(\nu, z) \quad (\mathrm{ED}) , \tag{22}$$

where

$$\mathscr{J}(\nu, z) = \int_z^\infty \left(\frac{1 + z}{1 + z'}\right)^3 f(z', z)(1 + z')(1 + 2q_0 z')^{-1/2} \times \exp\,[-\tau_{\rm eff}(\nu, z, z')] \frac{\tilde{f}_{\nu'}}{\tilde{f}_\nu} dz' , \tag{23}$$

and $\nu' = \nu(1 + z')/(1 + z)$. The generalization to the constant comoving CC case is trivial as the function f must be set equal to unity and the integral taken up to $z_{\rm on}$. Note that the integrated ionizing background is actually the sum of the direct radiation from the sources and the diffuse emission from radiative recombinations within the intercloud medium and the absorbing clouds. Since the intercloud medium is optically thin to UV photons, its contribution to the UV photoionizing field is negligible. We show in Appendix D that the estimated contribution of the diffuse emission from the clouds to the total photoionization rate is also negligible. Accordingly, we adopt $J(\nu, z)$ defined above as our estimate for the total metagalactic flux. It is instructive to express $J_{912}(z)$ in terms of the porosity parameter as

$$J_{912}(z) = \frac{h_P c}{4\pi} n_{\rm H,crit}(0) \Omega_{\rm IGM} \alpha_S (1 + q_0)(1 + z)^{1+q_0} \times \frac{\mathscr{J}_{912}(z) Q(z)}{1 - [(1 + z)/(1 + z_{\rm on})]^{1+q_0}} \quad (\mathrm{CC}) , \tag{24}$$

where $f_\nu \propto \nu^{-\alpha_S}$ is assumed for $\nu > \nu_L$ (so that $\xi = \tilde{f}_{\nu_L}/\alpha_S$). An approximation accurate to 15% over the range $3 < z < 6$ yields, for $\mu > 0.6$ and $z > z_*$,

$$J_{912}(z) \simeq \frac{h_P c}{4\pi} n_{\rm H,crit}(0) \Omega_{\rm IGM} \alpha_S (\mu + 0.38)(1 + z)^{2+q_0} \times \mathscr{J}_{912}(z) Q(z) \quad (\mathrm{ED}) , \tag{25}$$

for any z_*. The integral $\mathscr{J}_{912}(z) \equiv \mathscr{J}(\nu_L, z)$ depends primarily on the amount of intervening absorption and is rather insensitive to the spectral index of the photoionizing sources. In Table

[3] For reference, in the limit $z_{\rm on} \to \infty$, $Q(0)$ is equivalent to ζ, the dimensionless parameter defined in Shapiro & Giroux (1987).

[4] The specific energy radiated per unit time from a source of luminosity L_B in a band B centered at wavelength λ_B and of effective width $\Delta\lambda_{\rm eff}$, is $L_\nu = (\lambda_B/\Delta\lambda_{\rm eff})(\lambda_B/c)(f_\nu/f_{\nu_B}) L_B$, where f_ν is the spectral energy distribution of the radiating source. We define $\tilde{f}_\nu = L_\nu/L_B$.

TABLE 2

APPROXIMATIONS TO $\mathscr{J}_{912}(z)$ $(3 < z < 6)$

μ Range	$\mathscr{J}_{912}(z)$
Model LA	
CC $(\mu = 0)$	$0.65(1+z)^{0.5-q_0}$
$0.6 < \mu < 1.1$	$0.35(1+z)^{0.75-q_0}$
Model MA	
CC $(\mu = 0)$	$3.0(1+z)^{-(1+q_0)}$
$0.6 < \mu < 1.1$	$1.2(1+z)^{-(0.5+q_0)}$
Model HA	
CC $(\mu = 0)$	$1.9(1+z)^{-(1+q_0)}$
$0.6 < \mu < 1.1$	$2.15(1+z)^{-(1+q_0)}$

2 we present analytic approximations for $\mathscr{J}_{912}(z)$ in the models adopted, accurate to 15% over the redshift range $3 < z < 6$. For case ED, the fits may be extended to $z = 2$ with 20% accuracy. Equations (24) and (25) reflect the underlying physics of the ionization process: at least one UV photon is required per hydrogen atom to photoionize the IGM. A minimum value for the metagalactic flux at the present epoch is thus on the order of

$$\frac{h_P c}{4\pi} n_{\rm H,crit}(0)\Omega_{\rm IGM} = 3.3 \times 10^{-23}\,\Omega_{\rm IGM} h_{50}^2 \text{ ergs cm}^{-2}\text{ s}^{-1}\text{ Hz}^{-1}\text{ sr}^{-1}\,. \quad (26)$$

The porosity parameter Q is therefore an indication of the fraction of the critical amount of ionizing flux which has been supplied. Complete reionization is achieved for $Q(z_I) = 1$. However, in order to account for the low values of the Gunn-Peterson optical depth, photoionization equilibrium requires $Q(z)$ to take on larger values. Typically, equation (26) falls short of estimates for the metagalactic flux by a factor of a few tens to a few hundred. Thus, a plausible estimate for the porosity is $Q(z) \lesssim 100$. As will be shown below, this value suggests that if indeed radiating sources photoionized the IGM, they may have done so relatively recently in the history of the universe, possibly at an epoch that could soon be probed by QSOs. We shall discuss the observational consequences of this possibility in § 7.

We next derive a direct contraint on the epoch of reionization from limits on $\tau_{\rm GP}(z)$, valid in the approximation of negligible radiative recombinations. The Gunn-Peterson optical depth associated with resonant Lyα absorption at $\lambda_{\rm obs} = 1216(1+z)A$ is

$$\tau_{\rm GP}(z) = \left(\frac{\pi e^2 f_\alpha}{m_e \nu_\alpha H_0}\right) \frac{n_{\rm H\,I,D}(z)}{(1+z)(1+2q_0 z)^{1/2}}\,, \quad (27)$$

(Gunn & Peterson 1965), where $n_{\rm H\,I,D}$ is the H I density of the diffuse component, and all other symbols have their usual meanings. The optical depth is related to J_{912} through the condition of ionization equilibrium, which yields

$$\tau_{\rm GP}(z) = 0.15 h_{50}^{-1} T_4^{-0.75} (\Omega_D h_{50}^2)^2 (3+\alpha)(1+z)^5 \times (1+2q_0 z)^{-1/2} J_{-22}^{-1}\,, \quad (28)$$

where T_4 is the temperature of the ionized intercloud medium, and $J \propto \nu^{-\alpha}$ is taken as an approximation for the spectrum of the metagalactic flux at high z. It has been already pointed out that, as the effective optical depth $\tau_{\rm eff}$ diminishes with increasing frequency, a greater number of sources contributes to J for $\nu > \nu_L$, and the spectrum of the attenuated background is much harder than the local (stellar or QSO) emissivity: thus, $\alpha_S > \alpha$ (Bechtold et al. 1987; Miralda-Escudé & Ostriker 1990; Madau 1991). Combining equations (24) and (28), we find that the Gunn-Peterson optical depth and porosity are related by

$$\frac{\tau_{\rm GP}(z)Q(z)}{\Omega_D h_{50}^2} = 0.45 h_{50}^{-1} T_4^{-0.75} \left(\frac{\Omega_D}{\Omega_{\rm IGM}}\right) \times \frac{3+\alpha}{\alpha_S}(1+q_0)^{-1} \frac{(1+z)^{4-2q_0}}{\mathscr{J}_{912}(z)} \times \left[1 - \left(\frac{1+z}{1+z_{\rm on}}\right)^{1+q_0}\right] \quad \text{(CC)}\,. \quad (29)$$

From equation (25) we obtain instead

$$\frac{\tau_{\rm GP}(z)Q(z)}{\Omega_D h_{50}^2} \simeq 0.45 h_{50}^{-1} T_4^{-0.75} \left(\frac{\Omega_D}{\Omega_{\rm IGM}}\right) \frac{3+\alpha}{\alpha_S}(\mu + 0.38)^{-1} \times \frac{(1+z)^{3-2q_0}}{\mathscr{J}_{912}(z)} \quad \text{(ED)}\,. \quad (30)$$

Consider model CC with $z_{\rm on} = 6$, and take $\Omega_D = \Omega_{\rm IGM} = 0.02 h_{50}^{-2}$, $\alpha = 0.5$, and $\alpha_S = 0.7$. To obtain a temperature for the IGM, we integrate the time-dependent photoionization and radiative recombination equations together with the thermal energy equation for photoionization heating and cooling by radiative recombination losses, thermal bremsstrahlung, Compton cooling, and cosmological expansion, following Ostriker & Ikeuchi (1986), for the various QSO models and an IGM optically thin to UV photons. For $H_0 = 50$, we obtain a temperature at $z = 2.6$ of $T_4 = 0.62(0.46)$ for $q_0 = 0(0.5)$. Using attenuation model LA and equation (29), we find that $\tau_{\rm GP} < 0.05$ at $z = 2.6$ (Steidel & Sargent 1987b), requires $Q(z = 2.6) > 85(48)$ for $q_0 = 0(0.5)$. This implies, from equation (21), $z_I \gtrsim 5.9(5.8)$ for $q_0 = 0(0.5)$. Evolution model ED, with $\mu = 0.69$, requires instead $Q(z = 2.6) > 61(40)$ for $q_0 = 0(0.5)$. From equation (C1), we obtain $z_I \gtrsim 6.5(5.6)$ for $q_0 = 0(0.5)$. Therefore, in models based on QSO photoionization, the reionization epoch may have been as recent as $z_I \lesssim 6$. If radiative recombinations are important, as in model CM, the epoch of reionization may be even more recent. We discuss some observational consequences of this scenario in § 7.

5. OBSERVATIONAL CONSTRAINTS

In this section we summarize the current estimates of the Gunn-Peterson optical depth, which we use to further constrain the adopted models. Several groups have attempted to place limits on $\tau_{\rm GP}$ at high redshift. The methods employed have generally involved removing the contribution of intervening absorbers to the observed QSO flux deficit D_A (defined by Oke & Korycansky 1982 as the fractional decrement shortward of the Lyα emission line and longward of Lyβ), and attributing any residual amount to absorption by a diffuse component (Steidel & Sargent 1987b; Jenkins & Ostriker 1991). In addition to being related to $\tau_{\rm GP}$, the value of D_A itself provides a useful constraint on photoionization models at $z \gtrsim 4$.

Because of the uncertainty induced by the blue wing of the QSO Lyα emission line, Schneider, Schmidt, & Gunn (1991a)

define D_A only up to $\lambda = 1170$ Å in the QSO rest frame. Following the approach of Paresce et al. (1980), we take for the expected contribution D_L of the absorption lines to D_A

$$D_L = \left\langle 1 - \frac{I_\lambda^{\rm obs}}{I_\lambda} \right\rangle_L = 1 - \frac{1}{\Delta z} \int_{z_{\rm min}}^{z_{\rm max}} \exp\left[- \frac{dW_{\rm int}}{d\lambda} (1+z) \right] dz \,, \tag{31}$$

where $\Delta z = z_{\rm max} - z_{\rm min}$, $1 + z_{\rm min} = (27/32)(1 + z_{\rm em})$, $1 + z_{\rm max} = 0.9624(1 + z_{\rm em})$, and $z_{\rm em}$ is the QSO redshift. Here $dW_{\rm int}/d\lambda$ is given by

$$\frac{dW_{\rm int}}{d\lambda} = \frac{1}{\lambda_\alpha} \int_{W > W_{\rm min}} \frac{\partial^2 N}{\partial W \, \partial z} \, W \, dW \,, \tag{32}$$

where $\lambda_\alpha = 1216$ Å. In the presence of an intercloud medium, and when the volume filling factor of the absorbing clouds is much less than unity, the flux at any wavelength $\lambda = (1 + z)\lambda_\alpha$ is further reduced by a factor $\exp[-\tau_{\rm GP}(z)]$. The expression for the total decrement D_A is then given by modifying equation (31) to

$$D_A = \left\langle 1 - \frac{I_\lambda^{\rm obs}}{I_\lambda} \right\rangle = 1 - \frac{1}{\Delta z} \int_{z_{\rm min}}^{z_{\rm max}} f_{\rm II}(z) \times \exp\left[-\tau_{\rm GP}(z) - \frac{dW_{\rm int}}{d\lambda} (1+z) \right] dz \,, \tag{33}$$

where, in order to compare our photoionization models below with measurements of D_A at $z \gtrsim 4$, we have allowed for a filling factor $f_{\rm II}(z)$ of the ionized component less than unity. [The filling factor is related to the porosity by $f_{\rm II}(z) = Q(z)$ for $Q(z) < 1$ and $f_{\rm II}(z) = 1$ for $Q(z) > 1$.] In the limit $\tau_{\rm GP}(z) \ll 1$ [and $f_{\rm II}(z) = 1$], the Gunn-Peterson optical depth can be written as

$$\langle \tau_{\rm GP} \rangle \simeq \frac{D_A - D_L}{1 - D_L} \,, \tag{34}$$

where $\langle \tau_{\rm GP} \rangle$ is an average over the range $z_{\rm min} < z < z_{\rm max}$, weighted by $\exp[-(dW_{\rm int}/d\lambda)(1 + z)]$. If $\tau_{\rm GP}$ is nearly independent of z for $z_{\rm min} < z < z_{\rm max}$, then $\tau_{\rm GP} \simeq \log[(1 - D_L)/(1 - D_A)]$.

Schneider et al. (1991a) have estimated D_A for 34 QSOs with $3.1 < z < 4.9$. In the interval of redshift overlap ($3 < z < 3.4$), their values fall somewhat higher than those derived by Steidel & Sargent (1987a) on the basis of higher resolution data (6 Å compared to 25 Å). For the three Steidel & Sargent QSOs in this range, $\langle D_A \rangle = 0.26 \pm 0.02$, to be compared with the value for the 11 Schneider et al. QSOs in the same redshift interval, $\langle D_A \rangle = 0.41 \pm 0.02$, a deviation of 5 σ. None of the Schneider et al. QSOs has $D_A < 0.30$. Steidel & Sargent argue that there may be a tendency to overestimate the continuum in lower resolution data, thus overestimating D_A. At high redshift, we shall rely on the values of Schneider et al. to constrain our models. We caution the reader, however, that these values may be somewhat too high. In Appendix E we present our estimate of the Lyα cloud contribution, which provides a well-defined lower envelope to the D_A values.

Steidel & Sargent (1987b) find a 1 σ upper limit of $\tau_{\rm GP} < 0.05$ at $\langle z_{\rm abs} \rangle = 2.64$. (They take $\langle \tau_{\rm GP} \rangle = D_A - D_L$, which is correct in general only in the limits $\tau_{\rm GP} \ll 1$ and $D_L \ll 1$.) In a high-resolution study of Q2126−158, Giallongo, Cristiani, & Trevese (1992) have recently derived a 1 σ upper limit of $\tau_{\rm GP} < 0.04$ at $\langle z_{\rm abs} \rangle = 3$, based on a direct estimate of the quasar flux in regions of the spectrum where absorption lines are absent. For a large sample of QSOs, Jenkins & Ostriker (1991) have placed limits on $\tau_{\rm GP}$ at average emission redshifts $\langle z_{\rm em} \rangle = 3$ and $\langle z_{\rm em} \rangle = 4.2$. Formally, Jenkins & Ostriker cannot account for the measured D_A values using the known distribution of intervening absorbers, even at $z \sim 3$, where the properties of the Lyα forest are relatively well determined. Assuming the values for D_A have not been overestimated, these authors add an extra component, presumably arising from undetected very low column density systems, in order to match their value for D_A to the observations at $z \sim 3$. Even with this addition, they formally "detect" a Gunn-Peterson trough at $z \sim 4$, with $\tau_{\rm GP} \simeq 0.27$, which, given the uncertainties, is quoted as an upper limit. In the spectral range over which Jenkins & Ostriker measure D_A, the average absorption redshift is related to the average emission redshift by $\langle z_{\rm abs} \rangle = 0.915(1 + \langle z_{\rm em} \rangle) - 1$. Their 1 σ upper limits are therefore $\tau_{\rm GP} < 0.11$ for $\langle z_{\rm abs} \rangle = 2.7$ and $\tau_{\rm GP} < 0.31$ for $\langle z_{\rm abs} \rangle = 3.8$. Until the contribution of the Lyα forest to D_A is better determined, and higher resolution measurements of D_A itself are made, it will remain unknown whether their analysis has actually yielded a detection of Lyα resonant absorption from a diffuse IGM.

Adopting a method which does not rely on D_A, but uses instead the greater amount of information available available in the distribution of pixel intensities (see also Jenkins & Ostriker 1991), Webb et al. (1992) have reported a formal detection of $\tau_{\rm GP} = 0.04 \pm 0.01$ in their study of Q0000−263 ($z_{\rm em} = 4.1$). They restrict their analysis to the spectral range $5450 < \lambda < 6100$ Å, corresponding to $\langle z_{\rm abs} \rangle = 3.8$. Again, this result is sensitive to uncertainties in the Lyα forest parameters. Their results correspond conservatively to a 1 σ upper limit of $\tau_{\rm GP} < 0.05$.

6. PHOTOIONIZATION BY QUASARS

6.1. *The Integrated Ionizing Background*

According to recent surveys (e.g., Boyle, Shanks, & Peterson 1988), a pure luminosity evolution (PLE) model, in which QSOs statistically conserve their number since $z \simeq 2$, describes well the global properties of the quasar population at low redshifts. Beyond $z \simeq 2$, the comoving space density of quasars appears to stay constant up to a redshift of ~ 3 (see, e.g., Koo & Kron 1988; Boyle, Jones, & Shanks 1991; but see Hewett, Foltz, & Chaffee 1993, suggesting evolution up to $z \lesssim 3$). We adopt here (see also M92) the best fit to the QSO luminosity function (LF) for $0.3 < z < 2.9$ given by Boyle (1991):

$$\phi(L, z) = \frac{\phi^*}{L^*(z)} \left\{ \left[\frac{L}{L^*(z)} \right]^{\beta_1} + \left[\frac{L}{L^*(z)} \right]^{\beta_2} \right\}^{-1} \,, \tag{35}$$

with the entire LF shifting along the luminosity axis as the position of the break L^* evolves with redshift:

$$L^*(z) = L^*(0)(1 + z)^{k_L}, \quad z < z_c \,;$$
$$L^*(z) = L^*(z_c), \quad z > z_c \,. \tag{36}$$

Here z_c is the redshift at which the PLE switches off. In a cosmological model with $q_0 = 0.5$, $h_{50} = 1$, the best-fit values for the model parameters are $\phi^* = 7.1 \times 10^{-7}$ Mpc^{-3}, $\beta_1 = 3.9$, $\beta_2 = 1.5$, $k_L = 3.45$, and $z_c = 1.9$; the B magnitude at the break is $M_B^*(0) = -22.4$ at the present epoch. For $q_0 = 0.1$, we have $\phi^* = 3.8 \times 10^{-7}$ Mpc^{-3}, $\beta_1 = 3.8$, $\beta_2 = 1.6$, $k_L = 3.55$, $z_c = 2.1$, and $M_B^*(0) = -22.6$ (Boyle 1991). Following M92, we

shall assume a minimum luminosity of $L_{\rm min} = 0.017L^*$ at every epoch, or $y_{\rm min} = 0.017$ in the dimensionless emissivity integral ϵ introduced in § 4. For $q_0 = 0.5$, this corresponds to $M_{B_{\rm max}}(0) = -18$. At $z = 3$, $M_B^* = -26.4$, and $M_{B_{\rm max}} = -22$; thus we do not include quasars fainter than $B_{\rm max} \simeq 22.5$. Using these parameters, we find $\epsilon(q_0 = 0.1) \simeq 2.14$, and $\epsilon(q_0 = 0.5) \simeq 1.88$. Bright objects near L^* are the dominant contributors to ϵ; in the limit $L_{\rm min} \to 0$ the number density of QSOs diverges, but the emissivity increases by only 10%–20%. (The increase would be larger if the LF actually steepens at the faint end. See Hartwick & Schade [1990] for a discussion of QSO luminosity functions.)

The counts are more controversial above $z \sim 3$. It has been argued by Boyle (1991) and Irwin et al. (1991) that a model with a constant comoving space density of QSOs is consistent with the number of bright ($M_B < -26$) quasars at high z. However, according to Warren et al. (1991), a PLE model also fits the data over the range $2.2 < z < 3.3$, with the integrated space density $M_B < -26.3$ at $z \simeq 4$ being lower by a factor $\gtrsim 2.9$ ($q_0 = 0.5$) relative to $z \simeq 3$. The Warren et al. decline in space density is close to a factor $\simeq 2$ when compared with Boyle's $z \simeq 3$ LF. A decline in the LF is also seen at the low luminosities ($M_B \gtrsim -26$) probed by the Schmidt et al. (1991) grism survey: these authors require a factor of 3.2 decrease per unit redshift at $z > 3$ for $q_0 = 0.5$. We remark that these estimates are highly uncertain because of corrections for incompleteness and the adopted continuum emission spectrum.

To bracket the uncertainties, we will assume in the following two different models for the QSO global evolution at $z > 3$. First, we will follow Boyle (1991) (see also M92) and adopt a constant comoving number density of QSOs (case CC), with the $z = z_c$ LF providing an adequate description of the properties of the quasar population for $z_c \le z \lesssim 6$. If the decline at the faint end of the LF is indeed severe, this will provide an upper limit for the quasar contribution to the UV background. Second, an approximate lower limit to the integrated flux will be estimated following Warren et al. and imposing, for $z \ge z_* = 3$, a (luminosity-independent) decline in the LF by a factor of 2 per unit redshift (case ED). This corresponds to $\mu = 0.69$ in the exponential decay model of § 4.

We shall adopt the following model for the quasar spectral energy distribution:

Medium:

$$F_\nu \propto \begin{cases} \nu^{-0.7} & (\lambda > 1216\ \text{Å}); \\ \nu^{-1.5} & (\lambda < 1216\ \text{Å}). \end{cases} \tag{37}$$

This is based on observations reported by O'Brien, Gondhalekar, & Wilson (1988), and Sargent et al. (1989), and mimics fairly well the "medium" QSO spectrum used in Bechtold et al (1987), and "model QS2" of Miralda-Escudé & Ostriker (1990); its extrapolation to the soft X-rays is consistent with $\alpha_{\rm ox} \simeq 1.4$ (Zamorani et al. 1981). We shall also consider a harder spectrum given by

Hard:

$$F_\nu \propto \begin{cases} \nu^{-0.7} & (\lambda > 750\ \text{Å}); \\ \nu^{-1.1} & (130 < \lambda < 750\ \text{Å}); \\ \nu^{0.5} \exp(-0.4113\nu/\nu_L) & (60 < \lambda < 130\ \text{Å}); \\ \nu^{-0.6} & (\lambda < 60\ \text{Å}). \end{cases} \tag{38}$$

This is based partly on the "hard" spectrum of Bechtold et al., except that we extend the -0.7 frequency dependence observed for $\lambda > 1216$ Å to beyond the Lyman edge. In this case, $\alpha_{\rm ox} \simeq 1.2$.

In Figure 2 we show the estimated QSO contribution to the diffuse background at the Lyman edge. The metagalactic flux is given by $J_{-22}(z) = (3.5, 4.4)\mathcal{J}_{912}(z)f(z, \tilde{z})$ for both $q_0 = 0$ and

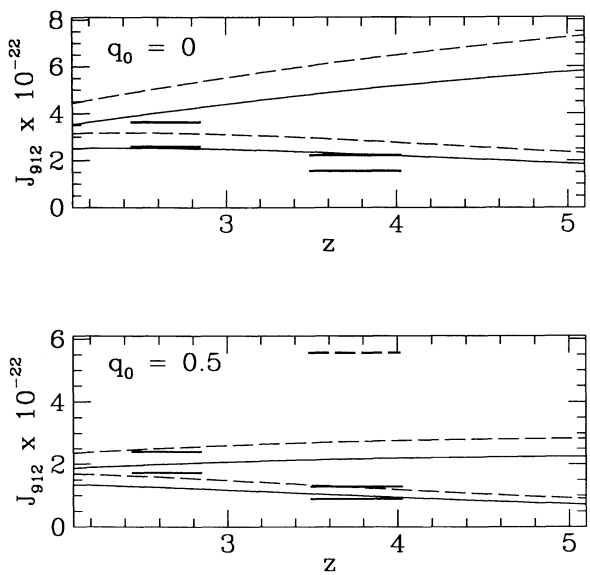

FIG. 2a

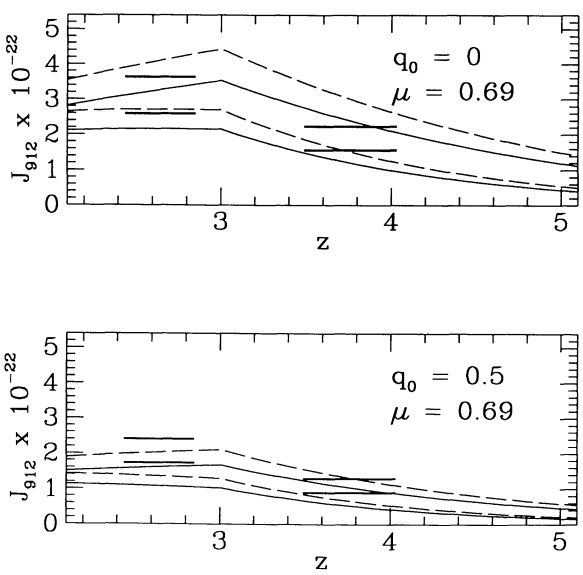

FIG. 2b

FIG. 2.—(*a*) Contribution of QSOs to UV background at the Lyman edge (constant comoving case). *Solid line:* medium spectrum; *dashed line:* hard spectrum. Upper pair is for low attenuation model (LA). Lower pair is for moderate attenuation model (MA). Horizontal bars are lower limits to J_{912} based on $\tau_{\rm GP}$ constraints and $\Omega_D h_{50}^2 = 0.02$. We show limits based on $\tau_{\rm GP}(\langle z_{\rm abs}\rangle = 2.6) < 0.05$ (*solid bars*), $\tau_{\rm GP}(\langle z_{\rm abs}\rangle = 3.8) < 0.31$ (*solid bars*), and $\tau_{\rm GP}(\langle z_{\rm abs}\rangle = 3.8) < 0.05$ (*dashed bar*). The upper (lower) bar in each pair corresponds to $H_0 = 50$ (80) km s^{-1} Mpc^{-1}. (*b*) Contribution of QSOs to UV background at the Lyman edge (exponential decay case). *Solid line:* medium spectrum; *dashed line:* hard spectrum. Upper pair is for low attenuation model (LA). Lower pair is for moderate attenuation model (MA). Horizontal bars are lower limits to J_{912} based on $\tau_{\rm GP}$ constraints, as in (*a*).

0.5, where the first and second values refer to the medium and hard spectral cases, respectively. (The $q_0 = 0$ universe is approximated by taking the results for $q_0 = 0.1$ from Boyle 1991). The results are independent of H_0 and only weakly dependent on q_0. For attenuation case LA, the flux is consistent with the proximity effect estimate of $10^{-21\pm0.5}$ ergs cm^{-2} s^{-1} Hz^{-1} sr^{-1} derived by Bajtlik et al. (1988), and lies only slightly below the proximity value for case MA. QSOs missing from surveys as a result of obscuration by dust in damped Lyα systems may increase the flux by an additional factor of 2 (Fall & Pei 1993), bringing it nearly into agreement with the best estimate from the proximity effect. We may compare our result with that of Miralda-Escudé & Ostriker (1992) for QSO model CC, attenuation model MA, and $q_0 = 0.5$ (the only case they consider). The agreement is good, although our estimate is a factor of 2 smaller for $z > 2.6$. This may be a result of the difference in luminosity functions. They base their estimate on a QSO luminosity function derived by extrapolating to high redshift the counts determined by Marshall (1985) for $z < 2.2$, while we use the directly observed counts for $z > 2$ as described by Boyle (1991).

The results of Figure 2 are well approximated using the fits in Table 2. For model LA, the fits yield, for $q_0 = 0$,

$$J_{-22}(z) \simeq (2.3, 2.8)(1+z)^{0.5}, \quad z > 3 \quad \text{(CC)}, \tag{39}$$

and

$$J_{-22}(z) \simeq (1.2, 1.5)(1+z)^{0.75} \times \begin{cases} 1, & 2.1 < z < 3, \\ \exp[-0.69(z-3)], & z > 3, \end{cases} \quad \text{(ED)}. \tag{40}$$

In a $q_0 = 0.5$ universe,

$$J_{-22}(z) \simeq (2.3, 2.8), \quad z > 3 \quad \text{(CC)}, \tag{41}$$

and

$$J_{-22}(z) \simeq (1.2, 1.5)(1+z)^{0.25} \times \begin{cases} 1, & 1.9 < z < 3, \\ \exp[-0.69(z-3)], & z > 3, \end{cases} \quad \text{(ED)}. \tag{42}$$

The approximations are accurate to 15% for $z > 3$, and, in model ED, to 20% for $1.9 < z < 3$. For $z < 2$, all models converge independent of QSO evolution and attenuation cases to the results of M92.

6.2. *Photoionization of a Smooth IGM (Case SM)*

The Gunn-Peterson limits on the background flux are shown in Figure 2 as pairs of horizontal bars, which extend over the redshift range over which the determinations are averaged. We take $\Omega_D h_{50}^2 = 0.02$ and assume $\Omega_{\mathrm{Ly}\alpha} \ll \Omega_D$; the role of the Ly$\alpha$ forest in the growth of the H II regions is then negligible. For the temperatures used in our estimates of the Gunn-Peterson limits, we use the results of the computations of the ionization and thermal histories from § 4. For $H_0 = 50$, we take $T_4 = 0.62$, (0.46) at $z = 2.6$, and $T_4 = 0.71$, (0.52) at $z = 3.8$, for $q_0 = 0$, (0.5). For $H_0 = 80$, the temperatures are $\sim$15% lower. In each pair, the upper (lower) bar in Figure 2 corresponds to $H_0 = 50$ ($H_0 = 80$). The most stringent constraints are provided at $z \simeq 2.6$. For attenuation model LA, both the constant comoving and the exponential decay cases are marginally consistent with the Gunn-Peterson limits for $H_0 > 50$, except for the $q_0 = 0.5$ ED case which requires $H_0 > 80$. For attenuation model MA, agreement requires $H_0 > 80$ and $q_0 = 0$. In Figure 3*a*, we show the porosity as a function of redshift in the exponential decay (ED) scenario. The breakthrough epoch ($Q = 1$) is in the range $4.9 < z_I < 6.4$. (For case CC, reionization occurs soon after the QSOs turn on at $z_{\mathrm{on}} = 6$.) The late epochs of reionization suggest the possibility that the IGM prior to breakthrough ($Q < 1$) may be probed by

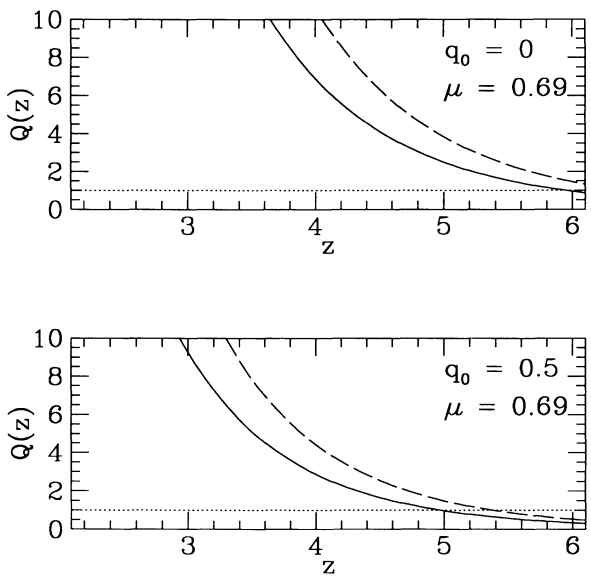

FIG. 3*a*

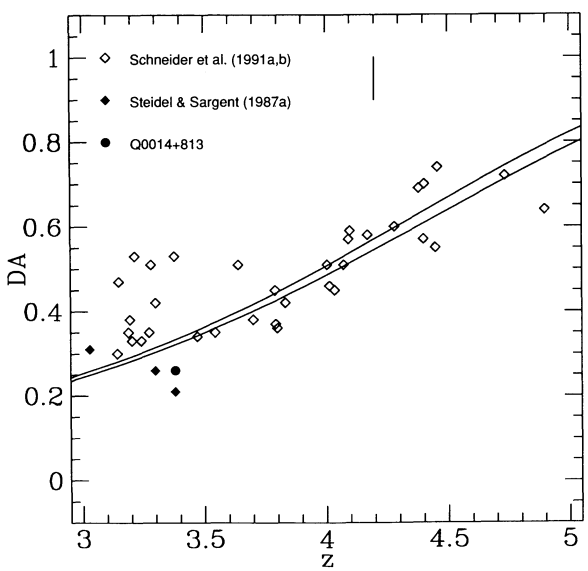

FIG. 3*b*

FIG. 3.—(*a*) Porosity $Q(z)$ for the cases of Fig. 2*b* for $\Omega_{\mathrm{IGM}} h_{50}^2 = \Omega_D h_{50}^2 = 0.02$. *Solid line:* medium spectrum; *dashed line:* hard spectrum. Complete reionization occurs for $Q(z) > 1$. Note that the epoch of reionization may be as recent as $z \sim 5$ in these models. Patches of un-ionized IGM would appear as absorption line systems in the spectra of high-redshift quasars for $Q(z) < 1$. (See § 7.) (*b*) The flux decrement D_A for the case of (*a*). The medium and hard spectral cases coincide. The lower line is for $q_0 = 0$ and the upper for $q_0 = 0.5$.

QSOs with $z \gtrsim 5$. A new class of H I absorption lines would appear in the spectra of these QSOs, arising from intervening patches of neutral, likely unprocessed material intercepting the QSO lines of sight. We discuss this intriguing possibility in the next section.

Because of the increasing value of the predicted τ_{GP} with redshift, we have checked that the limits imposed by the measurements of D_A are not violated. In model CC, the predicted values for D_A lie below the measured values. In model ED, the estimated values pass through the lower of the measured values, as shown in Figure 3*b*.

6.3. *Photoionization of a Clumped IGM (Case CM)*

If the limit $\tau_{GP} < 0.05$ at $\langle z_{abs} \rangle = 3.8$ set by Webb et al. (1992) is confirmed, all smooth IGM models (case SM) fail. It is possible instead that the IGM is highly clumped (case CM). In order to describe the evolution of the clumping factor with redshift, we will adopt the constant expansion rate model. In this scenario, clouds of different column density have different gas densities, and it is necessary to treat the cloudy component of the IGM as a multicomponent medium (see eq. [17]). The description can be simplified by noting that this is equivalent to a single component with an effective density

$$n_{\rm eff}(z) = \frac{1}{\Omega_{\rm Ly\alpha}\, n_{\rm H,crit}} \int n(z, M) n_p^2(M) \frac{\pi D^3}{6}\, dM\ , \qquad (43)$$

evolving as $n_{\rm eff}(z) = n_{\rm eff}(0)(1+z)^{3(1+q_0)}$. Here $n_p(M) = M/[(\pi/6)(1+4\chi)m_{\rm H} D^3]$. If $q_0 = 0$, then $n_{\rm eff}(0) \simeq 16\Omega_{\rm Ly\alpha} h_{50}^{-1} n_{\rm H,crit}(0)$ for $D(z = 2.5) \simeq 200$ kpc. In a $q_0 = 0.5$ cosmology, $n_{\rm eff}(0) \simeq 1.4\Omega_{\rm Ly\alpha} h_{50}^{-1} n_{\rm H,crit}(0)$ for $D(z = 2.5) \simeq 150$ kpc. In these models, radiative recombinations within the clouds significantly slow the growth of the individual H II regions.

We find that a model with $\Omega_{\rm IGM} h_{50}^2 = 0.04$ and $\Omega_D h_{50}^2 = 0.01$ ($\Omega_{\rm Ly\alpha} h_{50}^2 = 0.03$) does satisfy the Gunn-Peterson constraints. In the exponential decay model ED, the epoch of reionizaton is, however, very recent: $z_I = 4.8$–5.2 for $q_0 = 0$, and $z_I = 3.9$–4.2 for $q_0 = 0.5$, the range corresponding to a medium or hard QSO spectrum. (In case CC, the IGM is reionized by $z = 5$ for all models.) We show in Figure 4 the evolution of Q and D_A for these models. Despite a filling factor of ionized hydrogen less than unity for $q_0 = 0.5$, the constraints imposed by the meaurements of D_A are not violated by the exponential decay models (Fig. 4*b*). The absence of a Gunn-Peterson decrement in high-redshift QSOs rules out this scenario for $q_0 = 0.5$.

In a lower density medium, the epoch of reionization is slightly earlier. For $\Omega_{\rm IGM} h_{50}^2 = 0.025$ and $\Omega_D h_{50}^2 = 0.01$ ($\Omega_{\rm Ly\alpha} h_{50}^2 = 0.015$), the epoch of reionization becomes $z_I = 5.0$–5.4 for $q_0 = 0$, and $z_I = 4.1$–4.4 for $q_0 = 0.5$. The case for $q_0 = 0.5$, however, still appears problematic, as discussed in § 7 below.

6.4. *Photoionization of Pressure-Confined* Lyα *Clouds*

Alternatively, the intercloud medium may be collisionally ionized and hot, as discussed by, e.g., Ikeuchi & Ostriker (1986). In this scenario (which is similar to the clumpy IGM case discussed above, except that the Lyα clouds are assumed to be pressure-confined), we may still set useful constraints by asking whether QSOs are adequate for photoionizing the Lyα forest alone. Again, as recombinations within the Lyα clouds will significantly slow down the reionization process, it is necessary to model the cloud gas density. This is normalized at $z = 2.5$, according to equation (11). We take $q_0 = 0.5$, $h_{50} = 1$, and the redshift evolution exponent $x_1 = 5$ for pressure-confined clouds. We consider two cases, $\Omega_{\rm Ly\alpha} = 0.005$ and $\Omega_{\rm Ly\alpha} = 0.02$. If QSOs turn on suddenly at $z_{\rm on} = 6$ (model CC),

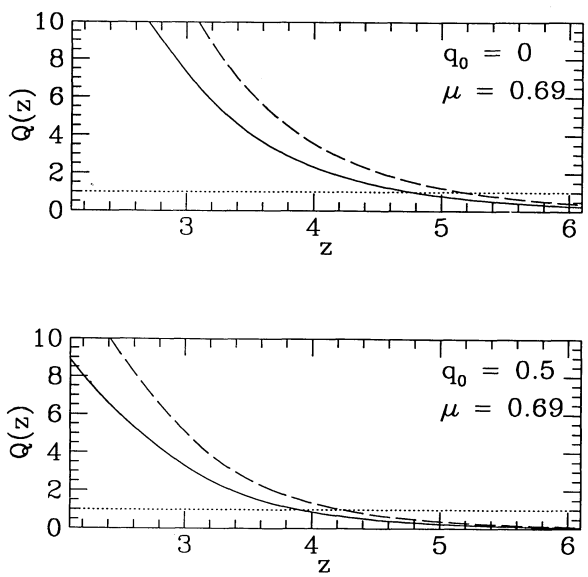

FIG. 4*a*

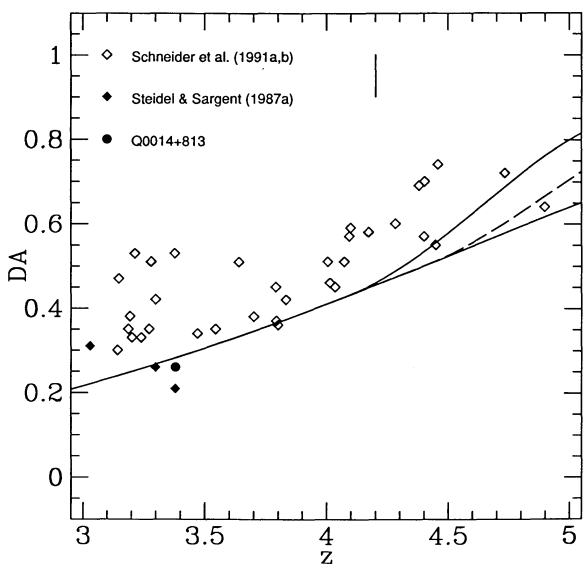

FIG. 4*b*

FIG. 4.—(*a*) Porosity $Q(z)$ for the cases of Fig. 2*b* for $\Omega_{\rm IGM} h_{50}^2 = 0.04$ and $\Omega_D h_{50}^2 = 0.01$. *Solid line:* medium spectrum; *dashed line:* hard spectrum. Complete reionization occurs for $Q(z) > 1$. Note that the epoch of reionization is in the range $3.9 \lesssim z \lesssim 4.2$ for $q_0 = 0.5$. The absence of broad absorption lines in the spectra of high-redshift QSOs arising from un-ionized patches of the diffuse intercloud medium for $Q(z) < 1$ rules out this scenario for $q = 0.5$ (see § 7). Intervening patches of un-ionized IGM would appear as absorption line systems in the spectra of high-redshift quasars for $Q(z) < 1$. (See § 7.) (*b*) The flux decrement D_A for the case of (*a*). *Solid lines:* medium spectrum; *dashed line:* hard spectrum. The lower line is for $q_0 = 0$ and the upper pair is for $q_0 = 0.5$. Despite the recent epoch of reionization for $q_0 = 0.5$, the constraint imposed by D_A is not violated.

TABLE 3

QSO PHOTOIONIZATION MODEL RESULTS

					$\tau_{GP}(2.6) < 0.05$					
					z_I		50		80	
$\Omega_{IGM} h_{50}^2$	$\Omega_D h_{50}^2$	$\Omega_{Ly\alpha} h_{50}^2$	q_0	MODEL	M	H	LA	MA	LA	MA
Smooth IGM (Case SM)[a]										
0.02	0.02	0	0	CC	5.8	5.8	Y	N	Y	M
0.02	0.02	0	0.5	CC	5.6	5.7	M	N	Y	N
0.02	0.02	0	0	ED	5.9	6.4	M	N	Y	M
0.02	0.02	0	0.5	ED	4.9	5.3	N	N	M	N
Clumped IGM (Case CM)[b]										
0.04	0.01	0.03	0	CC	5.6	5.7				
0.04	0.01	0.03	0.5	CC	5.1	5.4				
0.04	0.01	0.03	0	ED	4.8	5.2				
0.04	0.01	0.03	0.5	ED	3.9	4.2				
0.025	0.01	0.015	0	ED	5.0	5.4				
0.025	0.01	0.015	0.5	ED	4.1	4.4				
Pressure-confined Lyα Clouds										
0.005	0	0.005	0.5	CC	5.8	5.9				
0.005	0	0.005	0.5	ED	5.2	5.5				
0.02	0	0.02	0.5	CC	5.4	5.6				
0.02	0	0.02	0.5	ED	4.1	4.5				

[a] All models pass $\tau_{GP}(3.8) < 0.31$, but fail $\tau_{GP}(3.8) < 0.05$.
[b] All models pass $\tau_{GP}(2.6) < 0.05$ and $\tau_{GP}(3.8) < 0.05$.

they can photoionize the Lyα forest ($Q > 1$) by $z_I = 5.4$ in both cases. In the exponential decay model (case ED), we find that QSOs will completely photoionize the Lyα forest by $z_I = 5.2$ if $\Omega_{Ly\alpha} = 0.005$. For $\Omega_{Ly\alpha} = 0.02$, however, $Q = 1$ is not reached until $z_I = 4.1$–4.5, the exact value depending on the QSO spectral energy distribution. The absence of marked nonuniformities in the Lyα forest of high-redshift ($z > 4.5$) QSOs makes this last scenario marginal. Thus QSOs could easily photoionize the Lyα forest at $z < 5$ if the QSO comoving number density is constant and $z_{on} \lesssim 6$. If the source density decays beyond a redshift of 3, QSO photoionization of pressure-confined Lyα clouds appears more problematic.

We summarize the above results in Table 3. Under the z_I column, M and H refer to the medium and hard QSO spectral cases. Under the τ_{GP} column, Y denotes the model passes, N denotes failure, and M denotes marginal. The first and second entries in each pair refer to models LA and MA, respectively, for the amount of attenuation of the UV background.

6.5. *The* He II *Gunn-Peterson Test*

The He II Gunn-Peterson test at $\lambda_{obs} = 304(1 + z)$ Å could potentially provide stringent constraints on the intensity and spectrum of the UV background at short wavelengths. A low-density intercloud medium in ionization equilibrium with a QSO–dominated metagalactic flux will have a gas density ratio $n_{He\,II}/n_{H\,I} \simeq 1.8\ J_{912}/J_{228}$, with $n_{He} \simeq n_{He\,III}$. From equation (27) we derive

$$\frac{\tau_{GP}^{He\,II}(z)}{\tau_{GP}^{H\,I}(z)} \simeq 0.45\,\frac{J_{912}}{J_{228}}\,. \tag{44}$$

It would then be relatively easier to detect a Gunn-Peterson He II trough if the spectrum of the diffuse field is steep enough. Note that, in the case of an optically thin universe, $J_{912}/J_{228} = 8$ for $\alpha_S = 1.5$. If, however, absorption by intervening systems is taken into account, then $J_{912}/J_{228} \simeq 25$ for attenuation model MA (M92), and we would expect $\tau_{GP}^{He\,II}(z)/\tau_{GP}^{H\,I}(z) \sim 10$. This test, however, will suffer from the same complication shortward of the H Lyα emission line, namely the existence of a He II Lyα forest which will produce a decrement in the QSO flux shortward of 304 Å (rest frame).

7. IMPLICATIONS OF REIONIZATION

We have seen above that, under certain circumstances, QSOs can provide the UV radiation field required to satisfy conservative estimates of the constraints imposed by the Gunn-Peterson test at high redshift. A second requirement, however, is that QSOs complete their photoionization by $z \lesssim 5$, the redshift of the most distant observed objects. It is possible that the breakthrough epoch, when the H II region network has fully percolated, may have occurred at redshifts close to $z_I \sim 5$. Indeed, if QSOs turned on only at $z_{on} \sim 6$, or if their numbers decline with redshift at $z \gtrsim 3$, the epoch of reionization likely lies in the range $5 < z_I < 5.5$, a range which may well be probed in the not too distant future. In this section, we discuss the observational implications of detecting the intercloud medium prior to complete reionization.

What would be the observational signature of an IGM that was not completely reionized? Although I-front overlappings are common, the ambient medium remains neutral in the "walls" or interstices still present between the H II bubbles. The lines of sight to QSOs with $z > z_I$ will therefore intercept patches of neutral IGM which have not yet been engulfed by an H II region. These neutral interstices will give rise to a new class of absorption lines with column densities fixed by their sizes, and line widths given by the Hubble expansion across the patches. At redshifts just beyond z_I, these interstices will be small and the associated Lyα absorption lines will not differ

greatly from those associated with Lyman limit systems. As progressively deeper redshifts are probed, however, the lines will broaden as the neutral patches broaden, until they collectively form a Gunn-Peterson absorption trough shortward of the Lyα emission line. *In several of the QSO models described above, the lines would persist as distinct absorption features over an extended redshift interval of width $\Delta z \sim 0.5$–1, corresponding to $0.5 < Q < 1$, providing a unique probe of the epoch of reionization before the Gunn-Peterson trough is filled.*

A proper analysis of the IGM morphology and physical state at $z > z_I$ is beyond the scope of this paper. It would require a study of the complex geometry and cooperative interaction of overlapping H II spheres, as merging *I*-fronts propagate much faster into partially ionized regions. Also, with a distribution of turn-on redshifts, a new radiating source would have a probability $Q(z)$ of appearing within an already existing H II zone, thus precluding an analytic calculation of the resulting H II region. However, in the two limiting cases, $Q(z) \ll 1$ and $1 - Q(z) \ll 1$, we may estimate sizes, column, and number densities along lines of sight through the neutral patches.

The limit $1 - Q(z) \ll 1$ may be approximated by considering a toy geometrical problem, the "inverted" H II region: a neutral sphere embedded in the diffuse radiation field generated by the ionizing sources. The equation describing the rate at which the proper radius r_p of the patch shrinks with time is

$$4\pi r_p^2 n_{\rm H}(z)\left(\frac{dr_p}{dt} - Hr_p\right) = -4\pi r_p^2 \frac{2\pi J_{912}(z)}{\alpha h_P} . \quad (45)$$

The largest patches at a given epoch are the ones which will survive in a metagalactic field $J_{912}(z)$ just until the epoch of reionization z_I. Their size is then given for $z - z_I \ll (1 + z)$ by

$$r_p(z) \simeq \frac{2\pi J_{912}(z)}{H_0 n_{\rm H}(0)\alpha h_P}(1+z)^{-(5+q_0)}(z - z_I)$$

$$\simeq 0.23 h_{50}^{-1}\frac{\alpha_S}{\alpha}(1+q_0)\left(\frac{1+z}{6}\right)^{-4}$$

$$\times \frac{\mathcal{J}_{912}(z)}{1 - [(1+z)/(1+z_{\rm on})]^{1+q_0}}\left(\frac{z - z_I}{0.1}\right) {\rm Mpc} \quad ({\rm CC}) , \quad (46)$$

using equation (24) for $J_{912}(z)$ and taking $Q(z) \sim 1$. For $0.6 < \mu < 1.1$, we obtain, to 15% accuracy,

$$r_p(z) \simeq 1.4 h_{50}^{-1}\frac{\alpha_S}{\alpha}\left(\frac{1+z}{6}\right)^{-3}(\mu + 0.38)\mathcal{J}_{912}(z)$$

$$\times \left(\frac{z - z_I}{0.1}\right) {\rm Mpc} \quad ({\rm ED}) . \quad (47)$$

Note that the size of a patch is independent of the gas density of the intercloud medium. The corresponding average column density $\langle N_{\rm H\,I}\rangle = (4/3) n_{\rm H} r_p$ is

$$\langle N_{\rm H\,I}\rangle \simeq 8.8 \times 10^{18} h_{50}^{-1}\left(\frac{\Omega_D h_{50}^2}{0.02}\right)\frac{\alpha_S}{\alpha}(1+q_0)\left(\frac{1+z}{6}\right)^{-1}$$

$$\times \frac{\mathcal{J}_{912}(z)}{1 - [(1+z)/(1+z_{\rm on})]^{1+q_0}}$$

$$\times \left(\frac{z - z_I}{0.1}\right) {\rm cm}^{-2} \quad ({\rm CC}) . \quad (48)$$

For $0.6 < \mu < 1.1$, we find

$$\langle N_{\rm H\,I}\rangle \simeq 5.3 \times 10^{19} h_{50}^{-1}\left(\frac{\Omega_D h_{50}^2}{0.02}\right)\frac{\alpha_S}{\alpha}(\mu + 0.38)\mathcal{J}_{912}(z)$$

$$\times \left(\frac{z - z_I}{0.1}\right) {\rm cm}^{-2} \quad ({\rm ED}) . \quad (49)$$

The average velocity width of the corresponding Lyα absorption line is given by the Hubble expansion across the patch, $\langle \Delta V\rangle = (4/3) H_0 r_p (1+z)(1+q_0 z)^{1/2}$, or

$$\langle \Delta V\rangle \simeq 93\frac{\alpha_S}{\alpha}(1+q_0)\left(\frac{1+z}{6}\right)^{-3}(1+z)^{q_0}$$

$$\times \frac{\mathcal{J}_{912}(z)}{1 - [(1+z)/(1+z_{\rm on})]^{1+q_0}}$$

$$\times \left(\frac{z - z_I}{0.1}\right) {\rm km\ s^{-1}} \quad ({\rm CC}) , \quad (50)$$

for $q_0 = 0$ or 0.5. In the exponential decay model with $0.6 < \mu < 1.1$, we derive

$$\langle \Delta V\rangle \simeq 560\frac{\alpha_S}{\alpha}\left(\frac{1+z}{6}\right)^{-2}(1+z)^{q_0}(\mu + 0.38)$$

$$\times \mathcal{J}_{912}(z)\left(\frac{z - z_I}{0.1}\right) {\rm km\ s^{-1}} \quad ({\rm ED}) . \quad (51)$$

We note that the column density and velocity width will be correlated according to

$$\frac{N_{\rm H\,I}}{\langle \Delta V\rangle} = \frac{n_{\rm H}(z)}{H_0(1+z)(1+2q_0 z)^{1/2}} . \quad (52)$$

If n_p is the comoving number density of neutral patches, then the expected number of absorption lines detected per unit redshift along a line of sight would be $dN/dz \simeq (c/H_0) n_p \pi r_p^2 (1+z)/(1+2q_0 z)^{1/2}$. Noting that $(4\pi/3) n_p r_p^3 (1+z)^3 \simeq 1 - Q(z)$, and using the definition of $\langle \Delta V\rangle$, we derive

$$\frac{dN}{dz} \simeq \frac{c}{\langle \Delta V\rangle}\frac{1 - Q(z)}{1+z} . \quad (53)$$

As an example, consider the case of a clumpy IGM (model CM) photoionized by QSOs with a medium spectrum. If $q_0 = 0$, $\mu = 0.69$, $\Omega_D h_{50}^2 = 0.01$, and $\Omega_{{\rm Ly}\alpha} h_{50}^2 = 0.03$, then $z_I = 4.8$ (Table 3). We constrain this scenario using the $z_{\rm em} = 4.9$ QSO PC 1247+3406 (Schneider et al. 1991b). We adopt attenuation model LA, and take $\alpha \simeq 0.5$. At $z = 4.9$ we obtain $r_p \simeq 3\ h_{50}^{-1}$ Mpc, $N_{\rm H\,I} \simeq 5 \times 10^{19}\ h_{50}^{-1}$ cm^{-2}, and $\Delta V \simeq 1100$ km s^{-1}. For $Q(z = 4.9) = 0.87$, we expect a line density of $dN/dz \simeq 6$. Between $z = 4.8$ and 4.9, the expected number of lines would be $\lesssim 1$. Therefore we cannot rule out a reionization epoch as recent as $z_I = 4.8$ on the basis of the current observations.

The new population of absorption systems may be distinguished by their unique line profile. The lines will be black for $|\nu - \nu_\alpha| < (\langle \Delta V\rangle/2c)\nu_\alpha$, where ν is measured in the rest frame, just as in the Gunn-Peterson effect. In the wings, where $|\nu - \nu_\alpha| > (\langle \Delta V\rangle/2c)\nu_\alpha$, the profile function is

$$\phi(\nu) \simeq \frac{\Gamma}{4\pi^2 \nu_\alpha^2}\left[\left(\frac{\nu - \nu_\alpha}{\nu_\alpha}\right)^2 - \left(\frac{\langle \Delta V\rangle}{2c}\right)^2\right]^{-1} \quad (54)$$

in the limit $|\nu - \nu_\alpha| - (\langle \Delta V\rangle/2c)\nu_\alpha \gg \Gamma/4\pi$, where $\Gamma = (8\pi/3)(\pi e^2/m_e c)(\nu_\alpha/c)^2 f_{\rm lu} = 6.26 \times 10^8$ s^{-1} is the radiative damping constant for Lyα. At sufficiently high resolution, these features would therefore appear as damped Lyα systems, in

that the QSO flux would vanish over a finite width. The detailed profile, however, would not match the radiation damping profile. For low column density lines ($\log N_{\rm H\,I} < 10^{20}$ cm^{-2}), the mismatch would be especially conspicuous since the radiation damping core should not yet have appeared. A second distinguishing characteristic of the lines would be the absence of associated metal systems, assuming the IGM has not been contaminated by star formation at this early epoch.

If the observed QSO is radio loud, it may be possible to detect the 21 cm line in absorption from the patches. (A thorough discussion of the 21 cm signature of a neutral IGM is provided by Peebles 1971.) We consider the cases of a cold and a warm intercloud medium. By $z = 5$, the temperature of an adiabatically expanding IGM will be lower than the excitation temperature $T_{21} = 0.068$ K. However, it is also possible that a sufficiently small neutral patch ($\lesssim 100$ kpc) might be heated to temperatures larger than T_{21} by penetrating X- or cosmic rays which might fill the space between the advancing I-fronts of nearby QSOs (see Madau & Meiksin 1991). In either cases, the stimulated absorption and emission due to the cosmic background radiation field dominates over neutral hydrogen atom collisions in the epochs of interest, and statistical equilibrium applies. The energy levels are then in the ratio g_u/g_l, where $g_u = 3$ and $g_l = 1$ are the statistical weights of the upper and lower levels, respectively. The line profile function at line center is $\phi(\nu = \nu_{21}) = c/(\langle \Delta V \rangle \nu_{21})$, where $\nu_{21} = c/21$ cm. With the inclusion of stimulated emission, the optical depth at line center is

$$\tau_{21} \simeq \frac{1}{4} N_{\rm H\,I}(z) \left(\frac{\pi e^2}{m_e c}\right) f_{\rm lu} \left[\frac{h_P \nu_{21}}{k T_R(z)}\right] \left(\frac{c}{\langle \Delta V \rangle \nu_{21}}\right)$$
$$\simeq 0.00312\, h_{50}^{-1} \left(\frac{\Omega_D h_{50}^2}{0.02}\right) \left(\frac{1+z}{6}\right) (1 + 2q_0 z)^{-1/2}, \quad (55)$$

after using equation (52), and where $f_{\rm lu} = 5.75 \times 10^{-12}$ is the upward oscillator strength of the 21 cm transition. We normalize the cosmic background radiation temperature by $T_R(z) = 2.74(1 + z)$. Note that a measurement of the 21 cm optical depth of a patch would immediately yield $\Omega_D h_{50}$. For $|\nu - \nu_{21}| > (\langle \Delta V \rangle / 2c)\nu_{21}$, the line profile will again be described by equation (54), after replacing ν_α by ν_{21} and setting $\Gamma = 2.87 \times 10^{-15}$ s^{-1}. The neutral patches will also emit 21 cm radiation, with a brightness temperature of

$$T_B = \frac{1}{4} \frac{h_P c}{k} \left(\frac{\pi e^2}{m_e c} f_{\rm lu}\right) \frac{n_{\rm H}(0)}{H_0} (1+z)^2 (1 + 2q_0 z)^{-1/2}$$
$$= 0.0515\, h_{50}^{-1} \left(\frac{\Omega_D h_{50}^2}{0.02}\right) \left(\frac{1+z}{6}\right)^2 (1 + 2q_0 z)^{-1/2} \text{ K}. \quad (56)$$

In the limit $Q(z) \ll 1$, the H II regions will not have much overlapped. We present an approximate treatment of the patches based on geometric considerations in this case. The average proper width of an interstice is given by $\langle l_p \rangle \simeq (4/3)[(1 - Q)/Q] r_I$, where r_I is the proper radius of a typical H II sphere. The corresponding neutral hydrogen column density is then

$$\langle N_{\rm H\,I} \rangle \simeq \frac{4}{3} n_{\rm H}(z) \frac{1-Q}{Q} r_I$$
$$\simeq 3.8 \times 10^{20} \left(\frac{\Omega_D h_{50}^2}{0.02}\right) \frac{1-Q}{Q}$$
$$\times \left(\frac{r_I}{10 \text{ Mpc}}\right) \left(\frac{1+z}{6}\right)^3 \text{ cm}^{-2}. \quad (57)$$

The corresponding Lyα absorption lines will be velocity-broadened by the Hubble expansion across the patch, appearing black over a velocity width given by

$$\langle \Delta V \rangle \simeq \frac{4}{3} \frac{1-Q}{Q} H_0 r_I (1+z)(1 + 2q_0 z)^{1/2}$$
$$\simeq 4000\, h_{50} \frac{1-Q}{Q} \left(\frac{r_I}{10 \text{ Mpc}}\right) \left(\frac{1+z}{6}\right)$$
$$\times (1 + 2q_0 z)^{1/2} \text{ km s}^{-1}. \quad (58)$$

For a Poisson distribution of H II sphere centers, the distribution of patch sizes l_p is given, in the limit $Q \to 0$, by

$$\frac{\partial^2 N}{\partial z\, \partial l_p} \simeq \frac{c}{H_0 \langle l_p \rangle^2} \exp\left[-l_p/\langle l_p \rangle\right] (1+z)^{-2} (1 + 2q_0 z)^{-1/2}. \quad (59)$$

Integrating equation (59), and using equation (58), we obtain for the redshift distribution of the patches

$$\frac{dN}{dz} \simeq \frac{c}{\langle \Delta V \rangle} \frac{1}{1+z}. \quad (60)$$

In the case of a clumpy medium (CM), model ED with $q_0 = 0.5$ gives $3.9 < z_I < 4.4$ for the epoch of reionization. At $z = 4.9$, the porosity is $Q \sim 0.5$ for a hard spectrum. An L_B^* QSO that turned on at $z_{\rm on} = 6$ will create an H II region with a radius $r_I \sim 10$ Mpc by this epoch. The expected velocity width of a neutral patch would be $\langle \Delta V \rangle \sim 9500$ km s^{-1}, corresponding to an observed line width of $\Delta\lambda \sim 220$ Å. No such features are observed in the spectrum of QSO PC 1247+3406 at $z_{\rm em} = 4.9$, although only ~ 3 are expected from equation (60). No such broad features are observed in the lower redshift QSO spectra in Schneider et al. (1991a) either. Moreover, we would expect the presence of smaller H II regions corresponding to weaker sources as well. Thus, several, say 20 Å features corresponding to 1 Mpc H II regions would be expected in the $z = 4.9$ QSO spectrum and are not observed. It seems therefore unlikely that the epoch of reionization could be as recent as $z_I \lesssim 4.4$.

We emphasize that the results in this section are very general and not contingent on QSOs being the source of photoionization. They apply to any photoionization model by discrete sources.

8. CONTRIBUTION OF FAINT BLUE GALAXIES

How does the quasar contribution to the UV background compare with what is expected from other plausible candidate sources of photoionization? Deep CCD images down to $B \sim 27$ have revealed a high surface density of weakly clustered, faint blue galaxies (Tyson 1988; Lilly, Cowie, & Gardner 1991). While the bulk of the $B < 24$ population is represented by normal galaxies at $\langle z \rangle \simeq 0.4$, flat-spectrum objects constitute a significant fraction of the counts for $B \geq 24$; these might be young, star-forming galaxies, where high-mass stars produce metals and UV photons. Note that Steidel & Sargent (1989) have argued that the spectrum produced by main-sequence stars is too soft to explain the ionic abundances of heavy-element QSO absorption systems. (However, Madau 1991 has shown that the energy spectrum of a galaxy-dominated background, once attenuation is accounted for, is much flatter than the local stellar emissivity. This "hardening effect" is due to the wavelength dependence of the Lyman continuum absorption associated with cloudy material.)

The contribution of flat-spectrum galaxies to the background light at the present epoch is

$$J_B^G(0) = \int_{24}^{27} N(B) f_B \, dB \simeq 2.4 \times 10^{-21} \text{ ergs cm}^{-2} \text{ s}^{-1} \text{ Hz}^{-1} \text{ sr}^{-1}, \quad (61)$$

where $\log N(B) \simeq 0.45B - 6.55$ is the number count of objects per square degree and per unit magnitude (Tyson 1988), and $\log f_B = -19.34 - 0.4B$ is the observed flux at 4400 Å. The nature of this population of blue galaxies remains unclear. The large occurrence of gravitational lensing effects and the lack of any Lyman break candidates suggests that most of the objects are between $0.7 \lesssim z < 3$ (Tyson 1992; Guhathakurta, Tyson, & Majewski 1990). Now, the spectrum of a starbursting galaxy is relatively constant for $\lambda > 912$ Å, and decreases roughly as ν^{-1} at shorter wavelengths, $504 < \lambda < 912$ Å (Songaila et al. 1990); the Lyman-continuum break has a value of $D \simeq 3.5$ for a Salpeter IMF and a constant star formation rate. If only a fraction f_G of the population is actually forming stars at $z = z_{on}$, and the redshift distribution of this subpopulation is strongly peaked, then the contribution to the ionizing background at redshift z is

$$J_{912}^G(z) = J_B^G(0) f_G D^{-1} \frac{(1+z)^4}{(1+z_{on})} \exp\left[-\tau_{eff}(912, z, z_{on})\right], \quad (62)$$

provided $z_{on} < (4400/912) - 1$, and $(1+z) > (1+z_{on})\, 504/912$. A representative model with $f_G = 0.025$ and $z_{on} = 3$ yields

$$J_{912}^G(z) \simeq 10^{-21} \left(\frac{1+z}{4}\right)^4 \exp\left[-\tau_{eff}(912, z, z_{on})\right] \text{ ergs cm}^{-2} \text{ s}^{-1} \text{ Hz}^{-1} \text{ sr}^{-1}, \quad (63)$$

for $1.2 < z < 3$, an indication that faint, blue galaxies might indeed contribute to the high-z metagalactic flux if just a few percent of them are actively forming stars at early epochs. The model *fails* if a large fraction of the UV radiation emitted by massive stars cannot actually escape from the galaxies and is absorbed internally by neutral hydrogen or dust.

9. SUMMARY

We have investigated the case for photoionization of the IGM by quasars at high redshift. The conclusion of whether or not QSOs may provide the required metagalactic flux rests on several uncertain quantities related to the properties of the QSOs themselves and to the structure of the intergalactic medium. In this section, we outline our assessments of these uncertainties and summarize our results.

1. The degree of attenuation of the UV background by intervening absorption systems is made uncertain by the poorly known column density distribution of the absorbers. In particular, we find a significant underdensity of Lyα forest clouds in the range $15 < \log N_{H\,I} < 17$, based on data in the literature. This deficit, if confirmed, may be an indication that the high column density systems are Jeans unstable. Note that Lyα absorbers with optical depths at the Lyman edge close to unity are the most effective in attenuating the UV background. Taking this deficit into account revises upward the expected ionizing flux from QSOs by a factor of 1.5–3 relative to previous estimates.

2. We argue that the IGM may be highly clumped, and consider two models for the dynamics of the discrete absorbers. In one, the Lyα clouds are not confined and expand at a (constant) rate on the order of the average Doppler b value (hence they all have the same size at a given epoch). In the second, the Lyα clouds are pressure-confined by a hot (and therefore collisionally ionized), rarefied intercloud medium (hence they all have the same gas density at a given epoch). We weigh the Lyα forest and obtain $0.002 \lesssim \Omega_{Ly\alpha} h_{50} \lesssim 0.05$. The upper value is comparable to the expected cosmological baryon density of the universe. We therefore consider two models for the photoionization of the universe, a smooth IGM in which the Lyα clouds play a negligible role ($\Omega_{IGM} \sim \Omega_D$, where Ω_D is the density of the diffuse intercloud medium), and a clumpy IGM in which the Lyα forest dominates the baryonic density ($\Omega_{IGM} \sim \Omega_{Ly\alpha}$). We estimate $0.01 < \Omega_D < 0.04$ for $H_0 = 50$ and $0.005 < \Omega_D < 0.01$ for $H_0 = 80$.

3. There are large uncertainties in the estimated values of the Gunn-Peterson optical depth τ_{GP}. Those based on D_A, the flux decrement in the spectrum of a QSO between Lyα and Lyβ, are subject to uncertainties in the value of D_A itself. Indeed, the average value for D_A found by Steidel & Sargent (1987a) in the range $3 < z < 3.4$ is 5 σ lower than the average value in the same redshift range derived from Schneider et al. (1991a). Caution must therefore be exercised in estimating τ_{GP} from D_A.

4. The existence and amount of a decline in the comoving space density of low-luminosity QSOs at $3 < z < 5$ is also highly uncertain. We therefore consider two cases, a constant comoving model (CC) in which the QSO comoving number density is constant over the range $2 < z < z_{on} = 6$, and an exponential decay model (ED), in which the QSO comoving density declines by a factor of 2 per unit redshift for $z > 3$. We include the effects of attenuation by intervening absorbers and provide approximate analytic expressions which are reliable to 15% accuracy. Our principal results are as follows (see also Table 3).

a. Smooth IGM.—Both CC and ED models are consistent with $\tau_{GP} < 0.05$ at $\langle z_{abs} \rangle = 2.6$ and $\tau_{GP} < 0.31$ at $\langle z_{abs} \rangle = 3.8$, provided $\Omega_D h_{50}^2 \lesssim 0.02$ and $H_0 > 50$, although the agreement is often marginal for low H_0. Model ED with $q_0 = 0.5$ fails unless $H_0 > 80$. If $\tau_{GP} < 0.05$ at $\langle z_{abs} \rangle = 3.8$, as suggested by Webb et al. (1992), all models fail.

b. Clumped IGM.—The Webb et al. constraint can be satisfied only in a clumpy IGM. We consider $\Omega_D h_{50}^2 = 0.01$ with $\Omega_{Ly\alpha} h_{50}^2 = 0.03$ or 0.015. In the $q_0 = 0.5$ ED model, we find that the epoch of complete reionization is $z_I \sim 4$. The absence of substantial absorption shortward of Lyα in higher redshift QSOs rules out this scenario. Model ED with $q_0 = 0$ is successful, with $z_I \sim 5$. All constant comoving (CC) QSO models are able to reionize the IGM by $z_I \simeq 5$.

c. Pressure-confined Lyα clouds.—If the intercloud medium is collisionally ionized and pressure-confines the Lyα clouds, we find that the QSOs photoionize the forest in model CC by $z_I \simeq 5$. QSO photoionization is marginal for model ED if $\Omega_{Ly\alpha} h_{50}^2 > 0.02$.

We conclude that, in several of the models studied, the observed QSOs alone can indeed provide the number of ionizing photons required at high redshifts to satisfy the observational constraints. We emphasize that the prevailing view in the literature, that additional sources of ionizing radiation were required at large redshifts (Bechtold et al. 1987; Shapiro & Giroux 1987; Miralda-Escudé & Ostriker 1990), was based on the suggested steep decline of the quasar population at $z \gtrsim 2.5$. The results of several recent multicolor surveys indicate that the comoving space density of QSOs in fact approaches near

constancy in the range $2 < z < 4$, thereby suggesting a reconsideration of the previous conclusions (also see M92; Miralda-Escudé & Ostriker 1992). At $z = 3$, we estimate the UV background at 912 Å provided by quasars, J_{912}, to be $2 < J_{912} < 6 \times 10^{-22}$ ergs cm^{-2} s^{-1} Hz^{-1} sr^{-1} for $q_0 = 0$ and $1 < J_{912} < 3 \times 10^{-22}$ ergs cm^{-2} s^{-1} Hz^{-1} sr^{-1} for $q_0 = 0.5$, close to the estimate of $10^{-21\pm0.5}$ ergs cm^{-2} s^{-1} Hz^{-1} sr^{-1} from the proximity effect (Bajtlik *et al.* 1988). The addition of objects possibly missed by QSO surveys because of obscuration by dust in intervening damped Lyα systems may increase the background by an additional factor of ~ 2 (Fall & Pei 1993), bringing it nearly into agreement with the proximity effect determination.

5. We find that the epoch of reionization for several successful models lies in the range $4.8 < z_I < 5.5$. This offers the possibility of probing the breakthrough era in the not too distant future, as higher redshift QSOs are discovered. We argue that a new class of absorption systems should appear in their spectra, with typical H I column densities of 10^{18}–10^{20} cm^{-2}, arising from neutral patches of primordial material not yet engulfed by the QSO *I*-fronts. The lines would have the appearance of damped Lyα systems in that the QSO flux would vanish over a finite velocity width, on the order of 1000 km s^{-1}, but they would be distinguishable from the damped systems by their unique line profiles, since the lines would be velocity-broadened by the Hubble expansion across the patches rather than by radiation-damping. These systems would be further distinguished by the absence of associated metal absorption lines. Detection of the 21 cm absorption features would permit a direct measurement of the density of the intercloud medium.

It is a pleasure to thank M. Fall, E. Giallongo, P. Shapiro, S. Tremaine, and especially C. Steidel for informative discussions and comments. A. M. was supported by an International Fellowship from the Natural Sciences and Engineering Research Council of Canada.

APPENDIX A

ESTIMATES OF $\Omega_{\rm Ly\alpha}$

1. PRESSURE-CONFINED MODEL

We will adopt the approach of Ikeuchi & Turner (1991) and Turner & Ikeuchi (1992) in discussing the pressure-confined model. These authors assume a population of spherical clouds with the same total hydrogen gas density $n_{\rm H,c}$ at a given epoch, $n_{\rm H,c} = n_{\rm H,c}(0)(1+z)^{x_1}$. (The results may be altered if large inhomogeneities in the IGM pressure are allowed.) The mass distribution follows a power-law, $n(z, M) \propto (1+z)^3 M^{-\delta}$. The comoving number density of clouds, $n(z, M)/(1+z)^3$, is constant, and the metagalactic flux at the Lyman edge evolves according to $J_{912} = J_{912}(0)(1+z)^j$. This mass distribution corresponds to the H I column density power-law distribution of equation (3), with $\beta = 3\delta - 4$, according to

$$\frac{\partial^2 N}{\partial z\, \partial N_{\rm H\,I}} = \frac{c}{H_0}(1+z)(1+2q_0 z)^{-1/2} \int_{M_{\rm min}}^{M_{\rm max}} dM n(0, M) 2\pi l(N_{\rm H\,I}, M) \left| \frac{dl}{dN_{\rm H\,I}} \right|_M , \tag{A1}$$

where $M_{\rm min} = (4/3)\pi(1+4\chi) m_{\rm H} n_{\rm H,c}(N_{\rm H\,I}/2n_{\rm H\,I})^3$, and $l(N_{\rm H\,I}, M)$ is the impact parameter in a cloud of mass M corresponding to a column density $N_{\rm H\,I}$. For $q_0 = 0$ or 0.5, the number of clouds above a threshold $N_{\rm H\,I,th}$ is given by $dN/dz = N_0(1+z)^\gamma$, where $\gamma = (5x_1/3 - j)\beta - 7x_1/3 + j + 1 - q_0$. An integration over the mas spectrum up to the maximum mass $M_{\rm max} = (\pi/6)(1+4\chi) n_{\rm H,c}(0) m_{\rm H} D_{\rm max}^3(0)$, which corresponds to an average (over all lines of sight) H I column density $\langle N_{\rm H\,I}\rangle_{\rm max} = (\frac{2}{3}) n_{\rm H\,I} D_{\rm max}$, yields

$$\Omega_{\rm Ly\alpha} = \frac{1}{2}\left(\frac{2}{3}\right)^\beta \frac{\beta^2 - 1}{2 - \beta} N_0 \left[\frac{3}{2} \frac{G_{\rm H} J_{912}(0) N_{\rm H\,I,th}}{(1+2\chi)\alpha_A(T) n_{\rm H,crit}^2(0)} \frac{H_0^2 D_{\rm max}(0)}{c^2}\right]^{1/2} \left[\frac{\langle N_{\rm H\,I}\rangle_{\rm max}(0)}{N_{\rm H\,I,th}}\right]^{-(\beta - 3/2)} . \tag{A2}$$

We emphasize that the coefficients $J_{912}(0)$, $n_{\rm H,c}(0)$, $D_{\rm max}(0)$, and $\langle N_{\rm H\,I}\rangle_{\rm max}(0)$ are introduced here only for the purpose of redshift scaling for $z \gtrsim 2$. They are not to be interpreted as the inferred values for these quantities at the present epoch, as the *Hubble Space Telescope* observations of 3C 273 (Bahcall et al. 1991) have indicated a different evolution for $z \lesssim 2$. In accordance with equation (2), we take $N_0 = 3.0$ for $N_{\rm H\,I,th} = 1.7 \times 10^{14}$ cm^{-2}. The contribution to $\Omega_{\rm Ly\alpha}$ is dominated by the most massive, hence largest, systems. Now, to estimate $\Omega_{\rm Ly\alpha}$ from equation (A2), we must specify the expansion rate. Ikeuchi & Turner (1991) have considered a model with $x_1 = 5$, where the hot, collisionally ionized medium expands adiabatically, while the photoionized clouds are kept isothermal. We adopt a maximum diameter of $D_{\rm max} = 400$ kpc at $z = 2.5$ from equation (15), and, following M92, take $j = -0.5$ and $J_{-22} = 1$. For $\beta = 1.5$ (1.7), we find $\Omega_{\rm Ly\alpha} \simeq 0.005$ (0.05) h_{50}^{-1}.

2. CONSTANT EXPANSION RATE MODEL

Consider now the constant expansion rate model, and again adopt a power law for the spectrum of cloud masses. We obtain $\delta = 2\beta - 1$, and the same expression for γ as in the pressure-confined model above. In this case, as long as $\beta > 3/2$, $\Omega_{\rm Ly\alpha}$ is

dominated by the *lowest* mass systems. If we denote the column density through the minimum mass clouds by $\langle N_{\rm H\,I}\rangle_{\rm min}$, then

$$\Omega_{\rm Ly\alpha} = \left(\frac{2}{3}\right)^{\beta} \frac{\beta^2 - 1}{2\beta - 3} N_0 \left[\frac{3}{2} \frac{G_{\rm H} J_{912}(0) N_{\rm H\,I,th}}{(1 + 2\chi)\alpha_A(T) n^2_{H,\rm crit}(0)} \frac{H_0^2 D(0)}{c^2}\right]^{1/2} \left[\frac{\langle N_{\rm H\,I}\rangle_{\rm min}(0)}{N_{\rm H\,I,th}}\right]^{-(\beta - 3/2)} . \tag{A3}$$

Taking $D = 150$ kpc and $\langle N_{\rm H\,I}\rangle_{\rm min} = 10^{13}$ cm^{-2} at $z = 2.5$ yields $\Omega_{\rm Ly\alpha} \simeq 0.07 h_{50}^{-1}$ for $q_0 = 0.5$, and $\Omega_{\rm Ly\alpha} \simeq 0.04 h_{50}^{-1}$ for $q_0 = 0$ and $D = 200$ kpc.

We remark that the ED model adopted for QSOs in § 6 may not be consistent with the simple evolution description above. For $z < 3, j > 0$ for this model, while for $3 < z < 4$, $\mu = 0.69$ corresponds to $j \sim -2.5$. Thus between $z < 3$ and $z > 3$, γ should increase by an amount $\Delta\gamma \sim 2$, much steeper than is observed. Such an increase could be largely cancelled by a flattening in the column density distribution at the low end: decreasing β by 0.1 results in a decrease of γ by an amount $\Delta\gamma \sim 1$. It is thus unclear how critical the disagreement is: the column density distribution is uncertain at a level of $\Delta\beta \sim 0.1$, and the simplifications above likely provide at best a crude approximation to the actual evolution and distribution of the absorbers. We adopt these simplified models in the absence of a definitive description of the Lyα forest systems.

APPENDIX B

EXPANDING H II REGIONS IN A MULTICOMPONENT MEDIUM

Here we derive the rate of ionizing photons which reach the *I*-front of an expanding H II region from a central ionizing source of radiation. We include the effect of absorption by a multicomponent medium, and use the notation of § 4.

The equation of ionization equilibrium for each component i is

$$4\pi n_{\rm H\,I,i} \int_{\nu_L}^{\infty} \frac{J_\nu}{h_P \nu} \sigma_\nu \, d\nu = (1 + 2\chi_i) n^2_{\rm H,i} \alpha_A(T_i) . \tag{B1}$$

Here, $J_\nu = J_{S,\nu} + J_{D,\nu}$, where $J_{S,\nu}$ is the mean intensity arising from the ionizing source, and $J_{D,\nu}$ represents the contribution arising from radiative recombinations within the absorbing media. Each component i is taken to have a He to H number ratio equal to χ_i, with both H and He fully ionized. The radiative transfer equation for the source intensity is

$$\frac{1}{r^2} \frac{d}{dr} (r^2 4\pi J_{S,\nu}) = -4\pi J_{S,\nu} \sigma_\nu \sum_i f_i n_{\rm H\,I,i} , \tag{B2}$$

where f_i is the volume filling factor of component i. The radiative transfer of the diffuse field is described instead by

$$\frac{1}{r^2} \frac{d}{dr} (r^2 4\pi J_{D,\nu}) = -4\pi J_{D,\nu} \sigma_\nu \sum_i f_i n_{\rm H\,I,i} + 4\pi \epsilon_{D,\nu} , \tag{B3}$$

where $\epsilon_{D,\nu} = \sum_i \epsilon_{D,\nu,i}$, and $\epsilon_{D,\nu,i}$ is the diffuse volume emissivity arising from each component i. This results from the radiative recombinations to the ground state of hydrogen in that component:

$$4\pi \int_{\nu_L}^{\infty} \frac{\epsilon_{D,\nu,i}}{h_P \nu} \, d\nu = f_i (1 + 2\chi_i) n^2_{\rm H,i} \alpha_1(T_i) . \tag{B4}$$

Adding equations (B2) and (B3), and integrating over $(d\nu/h_P \nu)$, we obtain

$$\frac{1}{r^2} \frac{d}{dr} (r^2 4\pi J_\nu) = -4\pi J_\nu \sigma_\nu \sum_i f_i n_{\rm H\,I,i} + 4\pi \epsilon_{D,\nu} = -\sum_i f_i (1 + 2\chi_i) n^2_{p,i} \alpha_B(T_i) , \tag{B5}$$

and using equations (B1) and (B4), and noting $\alpha_B = \alpha_A - \alpha_1$. The rate $S(r)$ of ionizing photons at distance r from the source is given by

$$S(r) = 4\pi r^2 \int_{\nu_L}^{\infty} \frac{4\pi J_\nu}{h_P \nu} \, d\nu , \tag{B6}$$

so that, on integrating equation (B5), we find

$$\begin{aligned} S(r) &= S(0) - \tfrac{4}{3}\pi r^3 \sum_i f_i (1 + 2\chi_i) n^2_{p,i} \alpha_B(T_i) \\ &= S(0) - \tfrac{4}{3}\pi r^3 \sum_i (1 + 2\chi) \Omega_i n_{\rm H,i} n_{\rm H,crit} \alpha_B(T_i) , \end{aligned} \tag{B7}$$

where Ω_i is the cosmological mass density of component i, $\Omega_i = f_i n_{\rm H,i}/n_{\rm H,crit}$. The critical density for a Friedmann cosmology, $\rho_{\rm crit}$, is related to $n_{\rm H,crit}$ by $n_{\rm H,crit} = \rho_{\rm crit}/(1 + 4\chi) m_{\rm H} = n_{\rm H,crit}(0)(1 + z)^3$, where $m_{\rm H}$ is the proton mass, and χ is assumed constant for all the components. For applications, we shall adopt $\chi = 1/12$.

APPENDIX C

POROSITY EVOLUTION FOR EXPONENTIAL DECAY MODEL

For the exponential decay model (case ED), the porosity $Q(z)$ can be expressed as

$$Q(z) = \Phi_*\left[\frac{L_*}{n_{\rm H}(0)H_0 h_P}\right]\frac{\xi\epsilon}{1+q_0}(1+z)^{-(1+q_0)}\mathscr{I}(q_0; z, z_*) , \tag{C1}$$

where

$$\mathscr{I}(q_0; z, z_*) = f(z, z_*) - \mu e^{\mu(1+z_*)}(1+z)^{1+q_0}\mathscr{F}[q_0; \mu, \text{Max}\,(z, z_*)] . \tag{C2}$$

Here,

$$\mathscr{F}(q_0 = 0; \mu, z) = E_1[\mu(1+z)] , \tag{C3}$$

and

$$\mathscr{F}(q_0 = 0.5; \mu, z) = 2(1+z)^{-0.5}\,[[\exp\,[-\mu(1+z)] - [\pi\mu(1+z)]^{0.5}\,\text{erfc}\,\{[\mu(1+z)]^{0.5}\}] . \tag{C4}$$

The asymptotic behavior of equation (C2) in the limit $\mu(1+z) \gg 1$ is

$$\mathscr{I}(q_0; z, z_*) \sim \frac{1+q_0}{\mu(1+z)}\exp\,[-\mu(z-z_*)] . \tag{C5}$$

For $\mu > 0.6$ and $3 < z < 6$, the range of interest in this paper, the limit $\mu(1+z) \gg 1$ is not in general met. An approximation accurate to 15% over this range is given by

$$\mathscr{I}(q_0; z, z_*) \sim \frac{1+q_0}{(\mu+0.38)(1+z)}\exp\,[-\mu(z-z_*)] . \tag{C6}$$

Using equation (C6), equation (C1) can be approximated to an accuracy of 15% for $\mu > 0.6$ and $3 < z < 6$, and for any $z_* < z$, by

$$Q(z) = \Phi_*\left[\frac{L_*}{n_{\rm H}(0)H_0 h_P}\right]\frac{\xi\epsilon}{\mu+0.38}(1+z)^{-(2+q_0)}\exp\,[-\mu(z-z_*)] . \tag{C7}$$

APPENDIX D

PHOTOIONIZATION RATE FROM LYMAN-ALPHA CLOUD RECOMBINATIONS

As already mentioned in Appendix B, the metagalactic flux J can be divided into two parts, a component J_S arising directly from discrete sources of photoionizaton such as QSOs, and a diffuse component J_D resulting from the emission associated with the highly ionized optically thin Lyα clouds, $J = J_S + J_D$. (Since the intercloud medium is optically thin, its contribution to the UV background is much less than that of the QSOs.) The contribution to the diffuse field from the much scarcer, optically thick Lyman limit systems can be neglected. In this Appendix, we demonstrate that the photoionization rate arising from the ground level recombinations of hydrogen atoms in the Lyα forest is also small, and $J \simeq J_S$.

Following equation (1), the diffuse radiation field from the Lyα clouds is given by

$$J_D(\nu, z) = \frac{1}{4\pi}\int_z^\infty\left(\frac{1+z}{1+z'}\right)^3\epsilon_D(\nu', z')f_c(z')\frac{dl}{dz'}\exp\,[-\tau_{\rm eff}(\nu, z, z')]dz' , \tag{D1}$$

where $dl/dz' = (c/H_0)(1+z')^{-2}(1+2q_0 z')^{-1/2}$ is the line element in a Friedmann cosmology, and $\epsilon_D(\nu', z')$ is the proper volume diffuse emissivity arising from radiative recombinations within an individual cloud at redshift z':

$$\epsilon_D(\nu', z') = \frac{2h_P\nu'^3}{c^2}\left(\frac{h_P^2}{2\pi m_e kT_c}\right)^{3/2}\sigma_{\nu'}\exp\left[\frac{h_P\nu_L}{kT_c}\left(1-\frac{\nu'}{\nu_L}\right)\right](1+2\chi)n_{{\rm H},c}^2(z') \tag{D2}$$

(e.g., Osterbrock 1989), which is strongly peaked at the threshold energy ν_L. Here, $f_c(z')$ is the volume filling factor of the clouds, assumed $\ll 1$, $n_{{\rm H},c}$ is the hydrogen gas density within a given cloud, and T_c is the cloud temperature. All other symbols have their usual meaning or have been defined in the text. Assuming photionization equilibrium, we can eliminate $n_{{\rm H},c}^2$ in favor of the total metagalactic flux $J(z, \nu)$:

$$4\pi n_{{\rm H\,I},c}\int_{\nu_L}^\infty\frac{J(\nu, z)}{h_P\nu}\sigma_\nu d\nu(z) = (1+2\chi)n_{{\rm H},c}^2(z)\alpha_A(T_c) . \tag{D3}$$

Combining equations (D1)–(D3), we obtain

$$J_D(\nu, z) = \int_z^\infty \left(\frac{1+z}{1+z'}\right)^3 \frac{2h_P \nu'^3}{c^2} \left(\frac{h_P^2}{2\pi m_e k T_c}\right)^{3/2} \exp\left[\frac{h_P \nu_L}{kT_c}\left(1 - \frac{\nu'}{\nu_L}\right)\right] \times \left[\int_{\nu_L}^\infty \frac{J(\nu, z')}{h_P \nu} \sigma_\nu d\nu\right] n_{\mathrm{H\,I},c}(z') f_c(z') \frac{dl}{dz'} \frac{\sigma_{\nu'}}{\alpha_A(T_c)} \exp\left[-\tau_{\mathrm{eff}}(\nu, z, z')\right] dz' . \quad \text{(D4)}$$

Now, $n_{\mathrm{H\,I},c}(z) f_c(z)$ is the volume-averaged density of neutral hydrogen from clouds at redshift z and is related directly to the observed column densities by

$$n_{\mathrm{H\,I}}(z) f_c(z) = \int_{N_{\mathrm{H\,I}}} \frac{\partial^2 N}{\partial N_{\mathrm{H\,I}} \partial z} N_{\mathrm{H\,I}} \frac{dz}{dl} dN_{\mathrm{H\,I}} . \quad \text{(D5)}$$

Finally, we obtain for the fractional photoionization rate by J_D

$$\theta(z) \equiv \frac{\int_{\nu_L}^\infty [J_D(\nu, z)/h_P \nu] \sigma_\nu d\nu}{\int_{\nu_L}^\infty [J(\nu, z)/h_P \nu] \sigma_\nu d\nu} \simeq \int_{\nu_L}^\infty \frac{2\nu^2 \sigma_\nu}{\alpha_A(T_c) c^2} \left(\frac{h_P^2}{2\pi m_e k T_c}\right)^{3/2} \int_z^\infty \exp\left[\frac{h_P \nu_L}{kT_c}\left(1 - \frac{\nu'}{\nu_L}\right)\right] \left\langle \frac{d\tau(\nu', z')}{dz'} \right\rangle \exp\left[-\tau_{\mathrm{eff}}(\nu, z, z')\right] dz' d\nu , \quad \text{(D6)}$$

where

$$\left\langle \frac{d\tau(\nu', z')}{dz'} \right\rangle \equiv \int_{N_{\mathrm{H\,I}}} \frac{\partial^2 N}{\partial N_{\mathrm{H\,I}} \partial z'} N_{\mathrm{H\,I}} \sigma_{\nu'} dN_{\mathrm{H\,I}} = A_0(10^{14}) \int_{N_{\mathrm{H\,I},14}} N_{\mathrm{H\,I},14}^{-\beta+1} (1+z')^\gamma \sigma_{\nu'} dN_{\mathrm{H\,I},14} , \quad \text{(D7)}$$

using the notation of Table 1. Here, we have assumed that J is nearly constant with z over the relevant attenuation length,[5] and that the internal temperature T_c is a constant for all clouds independent of redshift, $T_c = 20{,}000$ K. For the cloud models in Table 1, and $3 < z < 5$, we obtain $0.01 < \theta(z) < 0.1$.

APPENDIX E

LYMAN-ALPHA FOREST CONTRIBUTION TO D_A

In this Appendix, we estimate the contribution of the Lyα forest to the flux decrement D_A. The distribution of line rest equivalent widths follows an exponential for $W > 0.2$ Å

$$\frac{\partial^2 N}{\partial W \partial z} \propto \exp\left(-\frac{W}{W_*}\right)(1+z)^\gamma , \quad \text{(E1)}$$

where $W_* = 0.3$ Å (Murdoch et al. 1986). For $W < 0.2$ Å, the number of lines shows a sharp rise, which can be well fitted by a second exponential with $W_* = 0.07$ Å. Such an increase is to be expected in the case of a power-law column density distribution, as low column density systems lie on the linear part of the curve of growth. The value $W = 0.2$ Å corresponds to a 50% departure from linearity in the curve of growth. Note that we have assumed that the observed equivalent width distribution is a true representation of the actual one, with line blending not severely affecting its determination over the relevant redshift range. We caution, however, that this question has never been thoroughly investigated. Extrapolating the low equivalent width fit to $W = 0$, we obtain, for $\gamma = 2.4$,

$$\frac{dW_{\mathrm{int}}}{d\lambda} = 3.0 \times 10^{-3}(1+z)^{2.4} . \quad \text{(E2)}$$

In Figure 5 we show the contribution of equation (E2) to D_A, using equation (31). Also plotted for comparison are the D_A measurements of Schneider et al. (1991a), and Steidel & Sargent (1987a): Lyα clouds do indeed provide a lower envelope to the observed D_A values. It is unclear whether all the scatter above this line can be accounted for by the presence of a few high column density systems along the line of sight. In particular, the Schneider et al. points all fall well above the cloud contribution at $z \gtrsim 3$, though the curve runs through the points of Steidel & Sargent. The reality of the discrepancy must await determinations of D_A with higher resolution data. In any event, the D_A measurements of Schneider et al. provide upper limits to the actual values of D_A, and

[5] This is defined as the length beyond which ionizing sources will be strongly attenuated because of the intervening absorption term exp $(-\tau_{\mathrm{eff}})$. In redshift space, this corresponds to $\Delta z \simeq 0.2$ at $z \simeq 3$ in the case of model MA (M92).

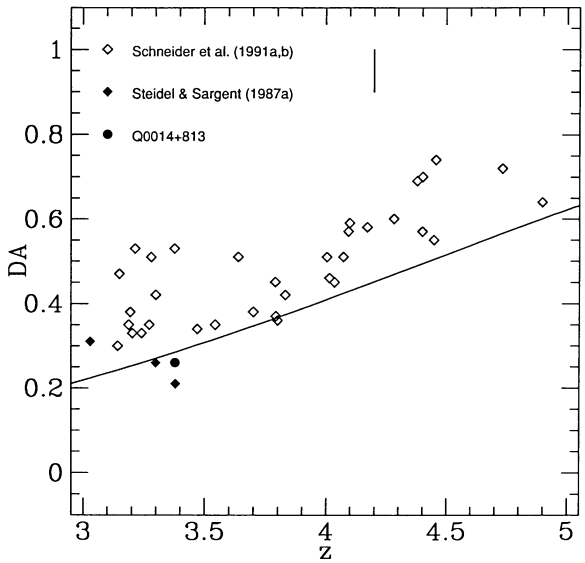

FIG. 5.—Measurements of D_A as determined by Schneider et al. (1991a, b) and Steidel & Sargent (1987a). The vertical line is the full 1 σ measurement error of ± 0.5 estimated by the authors. The solid line is the estimated contribution of the Lyα forest to D_A, according to eq. (E2). Also shown is a direct sum of the observed equivalent widths of Lyα forest lines detected in Q0014+813 by Rauch et al. (1992). Note that it lies very close to the expected value. Also note that it lies above the estimate of Steidel and Sargent for D_A for the same quasar.

will be used in the text. We also show an estimate for D_L by directly summing the observed equivalent widths of the absorption lines in the $z = 3.38$ quasar 0014+813 (Rauch et al. 1992). Restricting our range to $1050 < \lambda < 1175$ Å in the QSO rest frame, we find $D_L = 0.26$ from the Lyα lines alone. We display this point in Figure 5. Including the identified metal absorption lines increases this value to $D_L = 0.28$. Steidel & Sargent (1987a) estimate $D_A = 0.21 \pm 0.05$ for this object, less than the computed D_L value. (Note that this value of D_A appears to be a low excursion from their estimates for the remaining QSOs.) This gives a formal 2 σ upper limit of $\tau_{GP} < 0.03$ at $\langle z_{abs} \rangle = 3.0$. The reader should be cautioned, however, that the difference may arise from a difference in the continuum estimates of the observers. Properly, the same spectrum should be analyzed to determine D_A and the properties of the Lyα forest lines, with a consistent means of estimating the continuum.

REFERENCES

Arons, J., & Wingert, D. W. 1972, ApJ, 177, 1
Atwood, B., Baldwin, J. A., & Carswell, R. F. 1985, ApJ, 292, 58
Bahcall, J. N., Jannuzi, B. T., Schneider, D. P., Hartig, G. F., Bohlin, R., & Junkkarinen, V. 1991, ApJ, 377, L5
Bahcall, N. 1988, ARA&A, 26, 631.
Bajtlik, S., Duncan, R. C., & Ostriker, J. P. 1988, ApJ, 327, 570
Bechtold, J., Weymann, R. J., Lin, Z., & Malkan, M. 1987, ApJ, 315, 180
Boyle, B. J. 1991, in Texas/ESO–CERN Symposium on Relativistic Astrophysics, Cosmology and Fundamental Physics, ed. J. D. Barrow, L. Mestel, & P. A. Thomas (Ann. NY Acad. Sci., 647, 14)
Boyle, B. J., Jones, E. R., & Shanks, T. 1991, MNRAS, 251, 482
Boyle, B. J., Shanks, T., & Peterson, B. A. 1988, MNRAS, 235, 935
Carswell, R. F., Lanzetta, K. M., Parnell, H. C., & Webb, J. K. 1991, ApJ, 371, 36
Carswell, R. F., Morton, D. C., Smith, M. G., Stockton, A. N., Turnshek, D. A., & Weymann, R. J. 1984, ApJ, 278, 486
Carswell, R. F., Webb, J. K., Baldwin, J. A., & Atwood, B. 1987, ApJ, 319, 709
Chambers, K. C., Miley, G. K., & Van Breugel, W. J. M. 1990, ApJ, 363, 21
Donahue, M. J., & Shull, J. M. 1987, ApJ, 323, L13
Fall, S. M., & Pei, Y. C. 1993, ApJ, 402, 479
Giallongo, E., Cristiani, S., & Trevese, D. 1992, ApJ, 398, L9
Guhathakurta, P., Tyson, J. A., & Majewski, S. R. 1990, ApJ, 357, L9
Gunn, J. E., & Peterson, B. A. 1965, ApJ, 142, 1633
Hartwick, F. D. A., & Schade, D. 1990, ARA&A, 28, 437
Hewett, P. C., Foltz, C. B., & Chaffee, F. H. 1993, ApJ, 406, L43
Hughes, J. P. 1989, ApJ, 337, 21
Ikeuchi, S., & Ostriker, J. P. 1986, ApJ, 301, 522
Ikeuchi, S., & Turner, E. L. 1991, ApJ, 381, L1
Irwin, M., McMahon, R. G., & Hazard, C. 1991, in The Space Distribution of Quasars, ed. D. Crampton (ASP Conf. Ser. 21), 117
Jenkins, E. B., & Ostriker, J. P. 1991, ApJ, 376, 33
Koo, D. C., & Kron, R. G. 1988, ApJ, 325, 92
Lanzetta, K. M. 1991, ApJ, 375, 1
Lanzetta, K. M., Wolfe, A. M., Turnshek, D. A., Lu, L., McMahon, R. G., & Hazard, C. 1991, ApJS, 77, 1
Lilly, S. J., Cowie, L. L., & Gardner, J. P. 1991, ApJ, 369, 79
Lu, L., Wolfe, A. M., & Turnshek, D. A. 1991, ApJ, 367, 19
Madau, P. 1991, ApJ, 376, L33
———. 1992, ApJ, 389, L1 (M92)
Madau, P., & Meiksin, A. 1991, ApJ, 374, 6
Marshall, H. L. 1985, ApJ, 299, 109
Miralda-Escudé, J., & Ostriker, J. P. 1990, ApJ, 350, 1
———. 1992, ApJ, 392, 15
Murdoch, H. S., Hunstead, R. W., Pettini, M., & Blades, J. C. 1986, ApJ, 309, 19
O'Brien, P. T., Gondhalekar, P. M., & Wilson, R. 1988, MNRAS, 233, 801
Oke, J. B., & Korycansky, D. G. 1982, ApJ, 255, 11
Osmer, P. S. 1982, ApJ, 253, 28
Osterbrock, D. E. 1989, Astrophysics of Gaseous Nebulae and Active Galactic Nuclei (Mill Valley: University Science Books)
Ostriker, J. P., & Heisler, J. 1984, ApJ, 278, 1
Paresce, F., McKee, C., & Bowyer, S. 1980, ApJ, 240, 387
Peebles, P. J. E. 1971, Physical Cosmology (Princeton: Princeton Univ. Press)
Rauch, M., Carswell, R. F., Chaffee, F. H., Foltz, C. B., Webb, J. K., Weymann, R. J., Bechtold, J., & Green, R. F. 1992, ApJ, 390, 387
Sargent, W. L. W., Boksenberg, A., & Steidel, C. C. 1988, ApJS, 68, 539
Sargent, W. L. W., Steidel, C. C., & Boksenberg, A. 1989, ApJS, 69, 703
Sargent, W. L. W., Young, P. J., Boksenberg, A., & Tytler, D. 1980, ApJS, 42, 41
Schmidt, M., Schneider, D. P., & Gunn, J. E. 1986, ApJ, 306, 411
———. 1991, in The Space Distribution of Quasars, ed. D. Crampton (ASP Conf. Ser. 21), 109
Schneider, D. P., Schmidt, M., & Gunn, J. E. 1989, AJ, 98, 1507
———. 1991a, AJ, 101, 2004
———. 1991b, AJ, 102, 837
Shapiro, P. R. 1986, PASP, 98, 1014
Shapiro, P. R., & Giroux, M. L. 1987, ApJ, 321, L107
Smette, A., Surdej, J., Shaver, P. A., Foltz, C. B., Chaffee, F. H., Weymann, R. J., Williams, R. E., & Margain, P. 1992, ApJ, 389, 39
Songaila, A., Cowie, L. L., & Lilly, S. J. 1990, ApJ, 348, 371

Steidel, C. C. 1990a, ApJS, 72, 1
———. 1990b, ApJS, 74, 37
———. 1991, STScI Miniworkshop on the Reionization of the IGM, unpublished
———. 1992, private communication
Steidel, C. C., & Sargent, W. L. W. 1987a, ApJ, 313, 171
———. 1987b, ApJ, 318, L11
———. 1989, ApJ, 343, L33
Turner, E. L., & Ikeuchi, S. 1992, ApJ, 389, 478
Tyson, J. A. 1988, AJ, 96, 1
———. 1991, in Texas/ESO–CERN Symposium on Relativistic Astrophysics, Cosmology, and Fundamental Physics, ed. J. D. Barrow, L. Mestel, & R. A. Thomas (Ann. NY Acad. Sci., 647, 164)
Tytler, D. 1987, ApJ, 321, 49
Walker, T. P., Steigman, G., Schramm, D. N., Olive, K. A., & Kang, H. 1991, ApJ, 376, 51
Warren, S. J., Hewett, P. C., & Osmer, P. S. 1991, in The Space Distribution of Quasars, ed. D. Crampton (ASP Conf. Ser 21), 139
Webb, J. K., Barcons, X., Carswell, R. F., & Parnell, H. C. 1992, MNRAS, 255, 319
Wright, E. L. 1990, ApJ, 353, 411
Zamorani, G., et al. 1981, ApJ, 245, 357